Solar Energy 274 (2024) 112559

Contents lists available at ScienceDirect

Solar Energy

journal homepage: www.elsevier.com/locate/solener

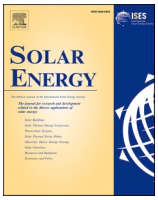

Exergy, exergo-economic, environmental and sustainability analysis of pyramid solar still integrated hybrid nano-PCM, black sand, and sponge

Usma Atiua Anika [a], Md. Golam Kibria [a,*], Shithi Dey Kanka [a], Md. Shahriar Mohtasim [a], Utpol K. Paul [a], Barun K. Das [b]

[a] Department of Mechanical Engineering, Rajshahi University of Engineering & Technology, Rajshahi-6204, Bangladesh
[b] School of Engineering, Edith Cowan University, Joondalup, WA-6027, Australia

ARTICLE INFO

Keywords:
Pyramid solar still
Desalination
Hybrid nanoparticles
Exergo-economic analysis
Sustainability

ABSTRACT

A sustainable and cost-effective technique for desalinating water with solar energy to alleviate the freshwater scarcity is the solar still. In this study, four different cases including the case-I: conventional solar still (CSS), case-II: CSS with fins and black sand, case-III: CSS with fins, hybrid enhanced nano PCM, black sand and sponges, case-IV: CSS with fins, hybrid enhanced nano PCM, crushed stone and sponges have been comprehensively investigated in terms of thermal, productivity, exergy, economic, environmental and sustainability point of view. The assessments were executed at the Rajshahi (latitude: 24°22′N, longitude: 88°36′E), Bangladesh. Later, the performance case-III was investigated by using river (Padma) water and discolored water, respectively. Average thermal efficiency on daily basis of case-III is about 32.44 % and 6.47 % higher than case-II and case-IV due to the improved heat storing configuration. In addition, cases-II, III, and IV all had exergy efficiency improvements of 18.89 %, 74.75 %, and 53.54 %, correspondingly in comparison to case-I. For cases I, II, III, and IV, the payback periods are 185, 159, 126, and 135 days, accordingly. In cases-I, II, III, and IV, modified SS results in cost-per-litre reductions of 73.5 %, 77.29 %, 81.89 %, and 80.63 %, correspondingly, as compared to market prices. Cases-I, II, III, and IV's energy production factors are 0.137, 0.099, 0.138, and 0.195 yr^{-1}, respectively. The research also supports the claim that adding fins, sponges, black sand, and hybrid enhanced nano-PCM to CSS results in a higher sustainability index.

Nomenclature

SS	solar still
CSS	conventional solar still
PCM	phase change material
HNPCM	hybrid nano-PCM
$\dot{E}_{ex,in}$	input exergy (W)
$\dot{E}_{ex,out}$	output exergy (W)
A_b	solar still area (m^2)
CRF	capital recovery factor
FAC	first annual cost ($)
SFF	sinking fund factor
ASV	annual salvage value ($)
TAC	total annual cost ($)
M	mean annual production (L/m^2)
E_{in}	embodied energy (kWh)
SS	total suspended solid (g/L)
TS	total solid (g/L)

(*continued on next column*)

Nomenclature (*continued*)

TDS	total dissolved solid (g/L)
N	life of solar still (year)
RWSS	reflector with solar still
X_{co_2}	co_2 emission (kg)
CCG	carbon credit gain ($)
SI	sustainability index
En_{annual}	annual total energy (kWh)
En_{out}	annual energy output (kwh)
h_{con}	convective heat transfer coe-efficient (W/m^2K)
h_{ev}	evaporative heat transfer coe-efficient (W/m^2K)
HCF	hollow circular fin
$\dot{m}_w$	freshwater productivity (kg/day)
h_{fg}	latent heat of evaporation (J/kg.k)
I_s	solar irradiation (W/m^2)
S	salvage value ($)
P	capital cost ($)
i	Interest rate (%)
AMC	annual maintenance cost ($)

(*continued on next page*)

* Corresponding author.
E-mail address: kibria@me.ruet.ac.bd (Md.G. Kibria).

https://doi.org/10.1016/j.solener.2024.112559
Received 9 January 2024; Received in revised form 25 March 2024; Accepted 22 April 2024

Nomenclature (*continued*)

CPL	cost per liter ($/L)
TS	total solid (g/L)
TDS	total dissolve solid (g/L)
TSS	total suspended solid (g/L)
EPT	energy payback time (yr.)
EPF	energy payback factor (yr.)$^{-1}$
MSS	modified solar still
T_s	sun temperature (K)
T_1	basin water temperature (K)
T_3	inner glass cover temperature (K)
T_4	ambient temperature (K)
Symbols	
η_{th}	thermal efficiency (%)
ε_{eff}	effective emissivity
η_{ex}	exergy efficiency (%)
μ_{co_2}	co_2 emission factor (Kg/kWh)
Subscripts	
Ex	regarding exergy as base
En	regarding energy as base

1. Introduction

A fresh water supply is one of the most essential needs for human beings. Pure drinking water is becoming less and less accessible. Globally, water scarcity is a terrible problem, particularly in rural and dry regions. While water makes up 71 % of the surface of our globe, the majority of it—roughly 97 %—is found in oceans and other salty waters [1]. Despite the fact that water covers two thirds of the planet, just 3 % of it is suitable for residential and drinking use [2]. Contaminated water is the source of many diseases in the human body. To meet the need for purified water, more sources of water transitioning from contaminated to its purest form should be used [3–7]. Furthermore, 2100 million people worldwide lack access to appropriately managed water, and more than 840 million people worldwide suffer from a shortage of freshwater, approximately 26.5 % of which is found in Africa [8]. In order to address the main issues facing the globe today, the United Nations (UN) has developed the 2030 Agenda for Sustainable Development (United Nations, 2021) [9]. As a fundamental necessity that is still unmet in most developing nations, Goal 6 aims to guarantee that everyone has access to clean water and sanitary facilities. Improvements in technology have led to the development of several desalination and water treatment techniques, such as thermal expertise (using multi-stage flash-MSF and multi-effect desalination-MED) and membrane expertise (using reverse osmosis-RO and electro-dialysis-ED) [2]. An endeavor to construct an affordable solar thermal desalination system that can be integrated into homes to provide drinkable water; likewise, the Asian continent, particularly the southern regions, acquires a lot of solar radiation that can be used to harvest renewable energy resources. Thus, because they are inexpensive and simple to make, solar stills are becoming more and more popular [10]. Consequently, using solar distillation to cleanse brackish or salted seawater is the most feasible way to address these water deficits. There are two categories for the solar still system: passive and active systems. While the active approach system is costly and unsuited for home usage, the passive method is straightforward, affordable, and simple to construct [11]. Unfortunately, the desalination process, also known as solar still (SS), has less productivity and dependability when it comes to meeting demand for water [12–14]. Arab alchemists employed stills for the first time in 1551, according to historical records. Over the following centuries, stills were used by further scientists and naturalists [15]. In the mining town of Las Salinas (northern Chile), Charles Wilson, a Swedish engineer constructed the very first “conventional” solar still plant in 1872 [16]. Solar-powered water distillation is based on straightforward yet effective concepts since distillation is akin to how nature purifies water. Water vapour is produced when solar radiation heats it to such a high degree. Which is left over after the liquid evaporates flows and condenses onto the glass’s face, ready to be collected. This treatment eliminates bacteria as well as impurities like salts and heavy metals. In the end, the water is purer than the rainiest water. It is also an extremely simple, low-maintenance, and eco-friendly device. It can be utilized in remote areas without power or access to a source of drinkable water [7,17–24]. Even though a single person needs about three liters of drinking water per day, solar still produces roughly 2.5–3.5 L of distillate per day at most. Due to the reduced output and decreased efficiency of solar stills, numerous researchers have worked with different techniques aimed at improving their output [26]. The present research takes into account a wide range of variables and changing of designs, which affect the SS’s productivity. With respect of Design, the pyramid and prism-shaped solar stills were particularly noteworthy, while square and triangular-shaped designs were possible. An analytical investigation on a pyramid-shaped solar still was conducted, and the results were compared with CSS [27]. The solar still’s surface area directly affects the rate of evaporation and condensation. In spite of this, pyramid solar still performs well and offers a larger surface area for the condensation process than basin solar [28]. The top cover of this kind of solar still has a shape akin to a pyramid, which is why the system is named pyramid solar still. It is more productive than a traditional still because it has a larger evaporative area for the same basin area. It can also be made more sophisticated by changing the cover angle, pyramid height, and other unique configurations. To harvest the most energy possible throughout the daylight hours, other types of solar distillers must be positioned such that their slanted surfaces face direct solar radiation and must be changed constantly as the sun moves across the sky [29]. But in the case of the pyramid solar still, this is not required. The side wall of the pyramid solar still casts far less shading on the water’s surface than the side walls of other traditional distillers generate [28]. Because the condensing area of a pyramid-shaped solar still is higher than that of other varieties, condensation in these sun stills is higher [30]. Numerous studies have shown that the added heat storage capacity of PCM and v-corrugated absorber plates can boost productivity in pyramid stills by up to 35 % and 88 %, respectively. Reflectors and mirrors, on the other hand, boost distillation production by up to 48 % and 53 %, respectively [31]. Furthermore, it is discovered that summertime radiation trapping using pyramid-type SS is more effective and captures more radiation than wintertime radiation trapping, which results in substantial reflection losses. Wick such as sponge materials, jute are used to increase the rate of evaporation, which raises the rate of freshwater production. Abu-Hijleh et al. [32] described a different approach for increasing the productivity of desalination by adding sponge cubes on top of the surface of the water. They found that this increased the distillation output by 18 %. Chauhan et al. [33] improved the evaporation process by using jute cloth in their research. A simple internal condenser, glass plate condensation, and PCM, also referred to as phage change materials, were used by Fath et al. [34] in a stepwise SS, and they discovered that this increased production yield by 5.2 kg/m^2/day. The mass transfer coefficient of evaporation for a passive single-slope desalination arrangement in a summer environment was thoroughly analysed by Tiwari & Tiwari. [35] in an attempt to ascertain the effect of water. The research found that the differences in the convective heat transfer coefficient for shallower water depths became less prominent. The temperature of the water and the absorber increased by 10 % and 12 %, respectively, when nanoparticles and black paint were used [36]. In diverse research, Sharshir et al. [37] used micro-flakes of copper oxide and graphite to improve the production of SS. The findings of their experiments indicate that the distillation output was higher with the use of these microflakes—by 44.91 % and 53.95 %, respectively—than with the use of traditional SS. Table 1 shows the summary of the recently conducted studies on solar still. According to Kandeal et al. [1], the modified solar still (MSS) in Case IV (ultrasonic atomizers were put on the MSSs basin) had the highest performance, particularly in terms of yield, with improvements in production, energy, and energy efficiencies of 113.72, 96.6, and 167.26 %, correspondingly. In accordance with Abdullah et al. [38], the reflector with solar still (RWSS’s) freshwater

Table 1
Summary of the recently conducted studies on solar still.

System Description	System Outcomes			Country	Ref.
	Thermal Efficiency	Exergy Efficiency	Daily Production (L/m^2/day)		
Assessment of a thermoelectric cooling system (12 W & 36 W) with a partly covered condensation lid in a passive solar still.	Improved by 44 %	Reduced by 25 %	Increased up to 126 %	Malaysia	[73]
Utilization of composite tablet prepared by activated carbon and metal powder (Cu, Al, and Fe).	Maximum 23 %.	Maximum 1.26 %.	Maximum 1.82.	Egypt	[74]
Evaluation of single slope solar still using sandblasting, milling, and shot-blast aided corrugation absorber plate.	Maximum 57.2 %.	Maximum 6.97 %.	Maximum 3.3 for shot-blast aided corrugation absorber plate.	India	[75]
Evaluation the thermophysical properties of the paraffin wax with Ag additives and application in stepped solar still and compared with PCM-SSS and CSSS.	–	–	Maximum 7.81–8.01 for NPCM-SSS.	India	[76]
Utilization of a sliding absorber plate in SS containing water. Case A comprises of water and insulation and water along with air stone and insulation for Case B.	28–42 % for Case-B and 27–39 % for Case-A.	–	2.8–4.2 for Case-B and 2.5–3.7 for Case-A.	Iran	[77]
Investigation of double solar still with the combination of fins, (PCM), external condenser (EC), and wick materials (WM).	Improved by 39.36 %.	Maximum 5.26 %.	Maximum 2.28.	Bangladesh	[78]
Utilization of modified parabolic concentrator integrated evacuated tube for single slope solar still.	50.8 %.	3.8 %.	5.4	India	[14]
Inner sidewall reflectors (ISR), hollow round fin (HCF), phase change material (PCM), and nanoparticle mixed PCM (nano-PCM) are used for assessing the effectiveness of a twin solar still.	121 %	111 %	Maximum 1.84.	Bangladesh	[79]
Utilization of evacuated thermal collector with angle in dual slope solar still under forced mode.	33.8 %	4.9 %	5.42	India	[80]
Evaluation the productivity of single slope solar still using PCM as thermal energy storage.	Increased annual energy savings by 10 % with PCM.	Increased annual exergy savings by 3 % with PCM.	In summer with PCM & without PCM 3.572 & 3.26 and in winter 2.2 & 2.126 respectively.	Egypt	[81]

production outperformed the conventional solar still's (CSS) by 300 % and 260 %, accordingly, with and without reflectors. RWSS and CSS have thermal efficiencies of 82 % and 35 %, respectfully. Al-Doori et al. [39] used crashing rocks, basalt rocks, and concrete bricks in three different methods to improve water output in a double-slope SS. The results show that the use of concrete bricks boosted waterproduction by an amazing 42 %. PCM-encapsulated cans in square and triangular designs were employed by Kannan et al. [40], who claimed significant advantages from PCM usage. Tanaka & Nakatake [41] examined how much sun energy a basin liner absorbs and how internal and external reflectors affect a single slope basins capacity to produce distillate water. The output rate was 21 % greater than the traditional SS across the whole year, according to the results. Additionally, the fin-nanoparticle designs in PCM-based thermal energy storage heat exchanger units were established by Abdulateef et al. [42]. According to the results of the experiment conducted by Kabeel et al. [43], the conventional pyramid solar panel still generates the most energy, 4.02 L/m^2/day, while the hollow solar panel with fins produces 5.75 L/m^2/day, a 43 % increase in daily output. The inclusion of PCM increases production to 8.1 L/m^2/day, or a 101.5 % increase in daily productivity. When MgO and TiO_2 nanofluids were utilized in a stepped solar still, Panchal et al. [44] discovered that the distillate yield rose by 45.8 % and 20.4 %, respectively. Tuly et al. [45] carried out a research project to look at the impacts of PCM, hollow cylindrical fins, and interior lateral reflecting combinations. They found that conventional productivity was boosted by up to 51.8 %, while productivity was further enhanced by 21.5 % when nanoparticles were mixed with PCM. In their investigation of a solar panel integrated SS system for supplying fresh water and electricity, Manokara et al. [46] found that insulation had the greatest energy and energy efficiencies, at 71.2 % and 4.5 %, respectively. According to research by Sharshir et al. [25], employing nanotechnology in tubular SS, such as ZnO nano-rod form, boosted production and efficiency by 30 % and 38 %, correspondingly. Several researchers have also used fins to boost the output and effectiveness of solar stills. Rabhi et al. [47] used a condenser and pin fin as an absorber in a solar still. The fins, which improve the absorbent surface inside the basin, and the condenser, which reduces heat losses, both contribute to the solar still's greater efficiency. Omara et al. compare the efficiency of a solar still with an external condenser coupled and a corrugated wick absorber surface [48]. Even so, the solar adjustment produces superior outcomes. The impact of several fin materials (aluminum, iron, copper, glass, stainless steel, mica, and brass) on the solar still's performance is examined by El-Sebaii and ElNaggar [49]. The productivity of the solar still is unaffected by fin material, according to the author's findings. The impact of fin height, thickness, and number on solar still performance was discovered by El-Sebaii et al. [50]. Fin height has the potential to enhance still performance, whereas fin thickness and quantity have the opposite effect. Manokar & Witson [51] constructed an acrylic solar still and added aluminum fins to the basin to lessen the bottom heat losses. The productivity of the modified solar still is greater than the traditional solar still. Jani & Modi. [52] used square and circular cross-section measurements to assess the efficiency of solar stills with fins. The outcome demonstrates that circular fins provide greater efficiency than square fins because of their increased surface area. A comparison of the solar still's performance with wick, sponge, and fins is made by Velmurugan et al. [53].

The conventional hemispherical solar still (CHSS), the hemispherical solar still with glass cover cooling (HSS-C), and the hemispherical solar still with CuO-water based nanofluid (HSS-N) were the three alternative designs of hemispherical solar distillers that were developed, produced, and tested by Attia et al. [54]. To find the optimal alteration, the conventional hemispherical still (CHSS) was used as the reference example. Three different concentrations of CuO nanoparticles (0.1 %, 0.2 %, and 0.3 %) were introduced to the basin water in the very first adaptation with the aim to improve the thermal characteristics of the basin fluid, improve the rate of water vapor generation beneath the distillation reservoir, and elevate the degree of solar energy consumed. The daily accumulative yield of HSS-N improves to 5.75 L/m^2/day, 6.40 L/m^2/day, and 6.80 L/m^2/day with enhancements 49.3 %, 66.2 %, and 76.6 % at volume fractions 0.1 %, 0.2 %, and 0.3 %, respectively, whereas the average daily progressive yield of CHSS is 3.85 L/m^2/day.

Experimental research on the thermo-economic performance of a hemispheric solar still outfitted with four different configurations was conducted by Sharshir et al. [55]. The investigation was conducted in four stages. Initially, a V-corrugated basin was employed in place of the distiller's flat basin. Second, a black cotton wick material was used to cover the corrugated basin. Thirdly, a wick-coated concave basin with paraffin wax containing phase change material (PCM) for latent thermal

storage. Ultimately, sheep fat PCM was used in place of paraffin. The best thermal performance and water productivity were demonstrated in the fourth instances. It produced 4737.5 mL/m^2/day with a thermal efficiency of 45 %. Additionally, there was a 39.75 % and 44.04 % improvement in the thermal performance as measured by the exergy and thermal efficiencies.

Based on thermodynamic, water yield, and economic analyses, a wide range of options, including tablet configuration (TC = full and staggered), metal weight ratio (MWR = 0 %, 5 %, 10 %, and 15 %), metal powder type (MPT = Fe, Al, and Cu), and water depth (WD = 1 cm, 1.5 cm, 2 cm, and 3 cm), were examined Said et al. [56] for their impact on the functionality of the system that was presented. For both full and staggered arrangement configurations, the use of composite tablets improves the solar still yield, energy, and energy efficiency by 18.5 %, 17.5 %, 202 %, and 44.1 %, 43.9 %, 29.1 %, respectively, while lowering costs by around 5.03 % and 21.9 %. Sharshir et al. [57] improved the hemispherical solar still (HSS) using corrugated copper, black cotton fabric, paraffin wax, sheep fat, graphite nanofluid, and graphite nanoparticles. Thermo-enviroecomonic indicators showed daily yield augmentation ratios of 43.3 %, 59.77 %, 78.77 %, and 95.2 % for the four cases.

According to the results, fins had the best effectiveness at 45 %, followed by sponge and wick at 29.3 % and 15.3 %, respectively. A few of the several factors affecting the efficiency of the solar still are the water depth in the basin, surrounding temperature, insulation thickness, basin material, humidity, solar radiation, wind speed, and inclination angle [25]. As a result, altering the design or operational parameters of the solar still can increase its efficacy and thermal performance. These include the double slope receiver [58], pyramid [59], spherical [60], tubular [61,62], stepped [63], and hemispherical solar stills [7], among others. Additional fins [7,52], internal and external reflectors [64], absorber plates [65], porous materials [66,67], wick materials [68], solar tracking [69,70], slope angles [71], cover cooling [72], and other features might all help achieve even greater increases. Some unaddressed research gaps are identified by an examination of prior studies and research from the literature review. Consequently, to increase PCM's thermal conductivity in solar stills, authors in the literature do not employ hybrid nanoparticle composites. Thus, it would be better if these open-ended problems were considered the problem at hand. However, prior trials using black sand as a viable heat storage below the absorber plate of solar stills have not been conducted. Thus, components that have never been used together in a system—like sponges, black sand, hybrid nano-enhanced PCM, and hollow circular fins—are integrated in a pyramid solar still. To increase the production of solar stills, a number of design changes have been suggested thus far and added many things to improve the conventional SS as represent in Fig. 1. While experimental investigation still plays a major role in information gathering and decision-making, researchers are now focusing on energy analysis, environmental analysis, heat transfer analysis, economic analysis, and sustainability analysis for evaluating and upgrading energy systems. Energy analysis helps thermal systems operate more efficiently by identifying and reducing losses and destructions inside the system. Furthermore, assessing an energy system's economic viability is crucial, and the payback period—a financial metric—is used to determine how long it takes to recover an initial investment. The following are the main contributions of this research:

- In this study, which is distinct from previous research, the effects of integrating hybrid nano PCM (HNPCM) into a modified pyramid solar still on freshwater productivity have been assessed. The pyramid solar still is modified using fins, sponge, black sand, ZnO, and Al_2O_3 nanoparticles are combined and added to PCM.
- A comparative analysis of heat transfer phenomena as well as the production yield has been investigated between the modified pyramid solar still in comparison with conventional solar still. Four different cases including the **case-I**: conventional solar still (CSS), **case-II**: CSS with fins and black sand, **case-III**: CSS with fins, hybrid enhanced nano PCM, black sand and sponges, **case-IV**: CSS with fins, hybrid enhanced nano PCM, crushed stone and sponges have been comprehensively investigated in terms of thermal, productivity, economic, and sustainability point of view. Firstly, saline water was used in all four cases, and a wide comparison in terms of thermal, productivity, economic, and sustainability points of view was made between them. Later, the performance of the modified solar still (case-III) was investigated by using river (Padma) water and discolored water, respectively.
- In order to assess the sustainability of the suggested system and the financial indicators of the modified pyramid solar still in comparison with the traditional scenario in order to ascertain its economic benefits, the study thoroughly looks at the various exergetic matrices, such as exergy efficiency and exergo-economic.
- In this experimentation process, the quality of the produced water is examined. The total solid (TS), total dissolved solid (TDS), and total

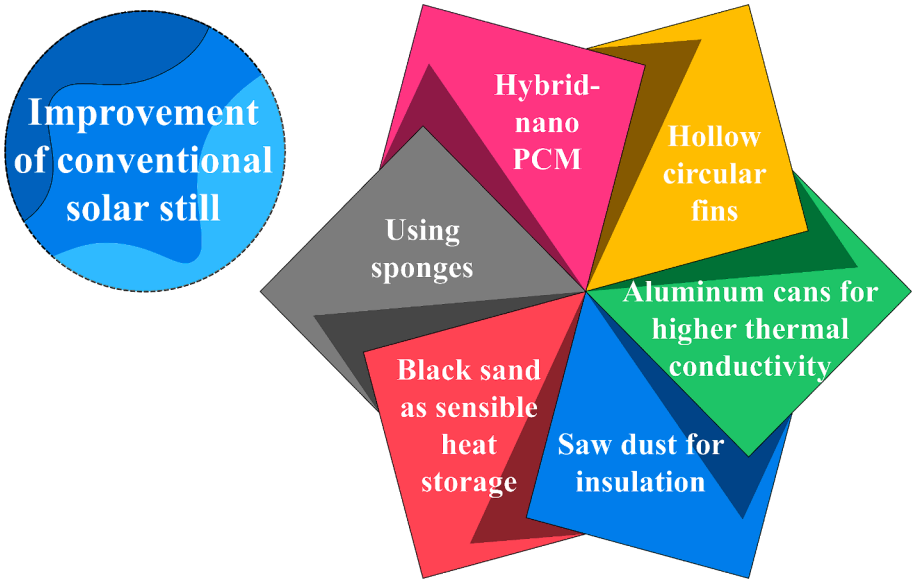

Fig. 1. Improvement of conventional SS.

suspended solid (TSS) of the produced water compared with the river water and discolored water

2. Methodology

This section encompasses the system description and specifications, recommended configurations along with their justifications, the procedure for fabricating hybrid nano-PCM, and the characterization of hybrid nano-PCM using samples.

2.1. System overview

An experimental setup consists of passive pyramid solar still was developed and constructed to assess the productivity of water by using fins, sponge, black sand, stones and Hybrid nano-PCM (HNPCM) in comparison with conventional solar still and to economical and exergy analyses on modified pyramid solar still with four different cases. At Rajshahi University of Engineering and Technology (in the Mechanical Engineering department), Rajshahi (Longitude/Latitude: 88.6241 E / 24.3636 N), the experimental investigation for the current research was carried out in September 2023. In Fig. 2, the schematic diagram of the proposed experimental setup is displayed. Temperature profiles, productivity, energy efficiency, and economic evaluation have been taken into consideration while evaluating and comparing the SSs' performance. Table 2 contains the dimensional parameters of the SS. The setup, controller, and data gathering system of the experiment were mounted on the roof of a shadow-free building. Saline water was feed to the SS by using a tank located about 1.2 m up from the ground to supply water at ambient temperature by using gravity. The whole area of the SS was 0.77 m^2. Because of the combined benefits of galvanized iron's resistance to corrosion, cost-effectiveness, heat-absorbing abilities, and the lifespan, the SS casing was constructed entirely of 0.004 m thick galvanized iron sheets. A glass cover of 0.003 m in thickness, 0.76 m^2 in area, and 0.30 m in height was taken into account. Glass cover which is thinner improves still productivity. According to the results of an experiment, the production rate of a basin-type solar still can be increased by 16.5 % by decreasing the thickness of the glass cover from 0.006 to 0.003 m [82]. The latitude of Rajshahi, Bangladesh (Longitude/Latitude: 88.6241 E/24.3636 N), was used to determine the inclination angle of the glass cover. The research study found that tilting at the identical angle as latitude enhanced efficiency by 63 % compared to alternative inclinations [79]. Consequences, the inclination angle of pyramid faces was taken as the same as latitude, 24°. The dimensional area of absorber plate was taken 0.25 m^2 with the thickness of 0.006 m. To enhance the absorption of solar energy intended for the absorber plate through the glass cover, the absorber plate was painted black. The majority of the thermal energy is reached to water mass after solar radiation is absorbed at the blackened surface, with a fractional amount being lost to the atmosphere through the bottom and sides. Sawdust was used to provide an insulation layer with a thickness of 0.04 m to prevent side and bottom losses because sawdust is relatively cheap, available and has good insulation property, it was preferred. Utilizing thermal insulation up to a thickness of 60 mm and asymptotically after that has a considerable negative impact on the still's production [83] and so 0.04 m was taken for the design of passive solar still.10 kg black sand was

Table 2
Dimensional parameters of the SS.

Parameter	Dimension description
SS body	0.77 m^2 (area)
Glass cover	0.76 m^2 (area), 0.003 m (thickness), 0.30 m (height)
Absorber plate	0.25 m (area), 0.006 m (thickness)
Black sand / stone holder	0.25 m (area), 0.006 m (thickness)
Hollow circular fin (81 no's)	0.01 m (height), 0.001 m (thickness), 0.1 m (pitch separation)
Insulation (sawdust) thickness	0.04 *m*
Cubic sponge	0.03 *m*
Aluminum can	0.056 m (diameter), 0.136 m (height)

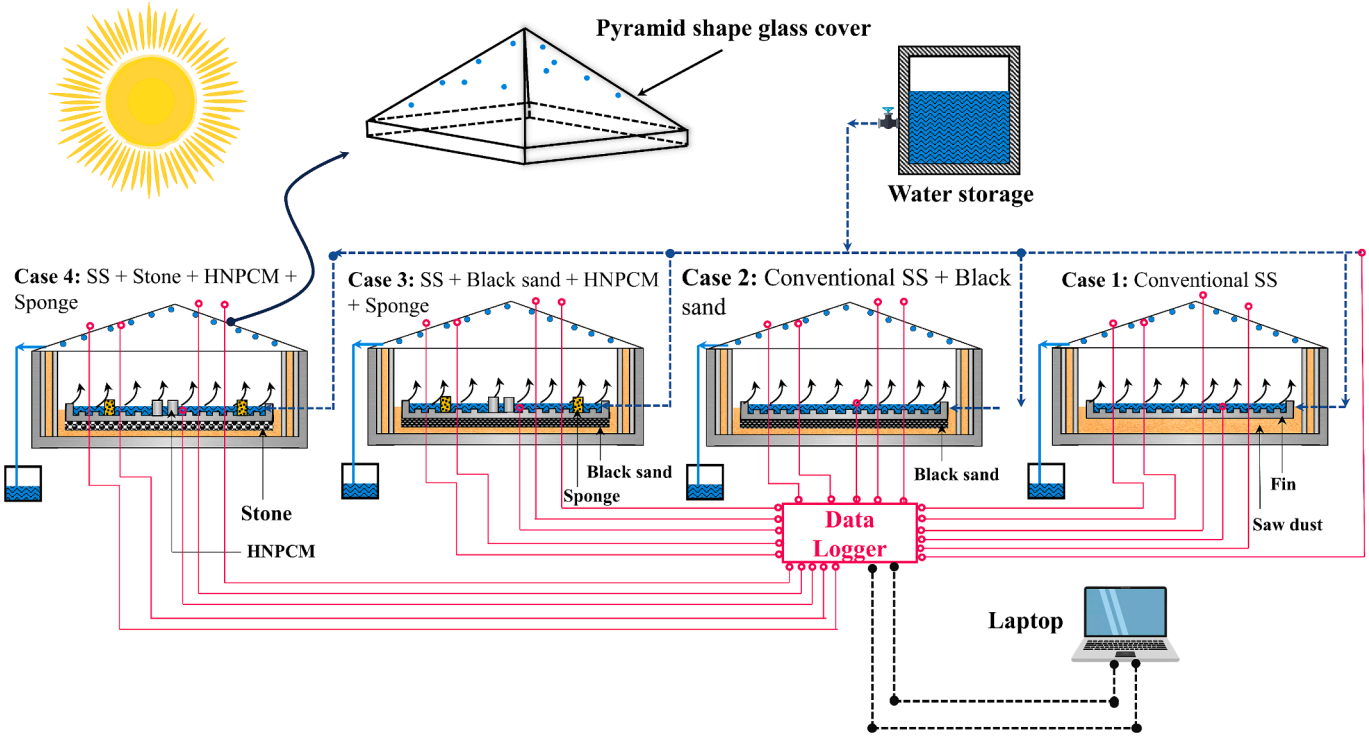

Fig. 2. Schematic layout of the experimental setup.

used as a sensible heat storage to absorb bottom heat loss from the basin, stored the thermal energy during the sunlight and liberated store energy to the basin water at the absence of solar radiation to enhance the daily average productivity of SS. In a different case, 3 kg of grey limestone was substituted for black sand in order to observe and evaluate the impact of employing stone as a sensible heat storage on the productivity of the SS. The mechanical and chemical properties, along with the size of the grey limestone used in the present study, are represented in Table 3 [84]. In this study, 81 hollow circular fins (HCF), each measuring 0.001 m in thickness and 0.01 m in height were used. The fins consisted of galvanized iron sheets with an exterior diameter of 0.01 m, and there was a 0.1 m pitch spacing between each subsequent HCF. Since they increase the SS basin's surface area and improvement in transferring heat between the absorber plate and basin water, HCFs are preferable over solid fins because the basin water is in direct contact with the larger surface areas of the HCFs both inside and outside heat transmission increases. In order to allow HCFs to submerge in the water and increase the heat transfer coefficient, the basin water was kept at a constant 20 mm water depth. Each aluminum can has a height of 0.136 m and a volume of 3.3×10^{-4} m, thus the maximum amount of paraffin wax with a mass density of roughly 900 kg/m^3 [85] stored in each can is 0.3 kg. Therefore, four aluminum cans held a total of 1.2 kg. In this study, 1.2 kg paraffin wax was used as a latent heat storage source to increase the daily productivity of modified SS. Because of its high latent heat of fusion, consistent melting properties, chemical stability, nontoxicity, affordability, and assurance, paraffin wax is chosen as a PCM storage media [81]. ZnO and Al_2O_3 nanoparticles were mixed in paraffin wax at weight ratios of 2 wt% and 2 wt%, respectively to prepare hybrid nano enhanced PCM. In order to increase paraffin wax's thermal conductivity and shorten PCM's charging-discharging time, ZnO and Al_2O_3 nanoparticles were added to PCM. After the preparation of hybrid nano enhanced PCM, it was loaded in four aluminum cans of height 0.136 m due to the availability and cost effectiveness of aluminum can and placed on the top of the absorber plat and submerged in basin water. Aluminum has high thermal conductivity and for this reason heat will transfer far faster through conduction from basin water to the hybrid nano enhanced PCM.

The paraffin wax melts when energy from the briny water is transferred through the can's wall. Cans containing paraffin wax are heated simultaneously, raising the temperature to facilitate faster melting and longer discharging times. The energy contained in paraffin wax's inner core releases heat during the release of heat to the water in order to increase the temperature and speed of evaporation. The aluminum cans were placed in square shaped on the absorber plate. It has been noted that the triangle pattern indicates a lower water temperature than the square design [86]. The bulk of paraffin wax may be the cause of this. Additionally, the area's increased exposure allowed heat from PCM cans to be transferred to the surrounding water in an equilibrium. In order to increase daily production, four 0.03 m long cubic sponges were used. These sponges reduce the volumetric heat capacity of the water in the absorber plate and maximize the temperature differential between the water's surface and the cooling glass cover. Sponge employs capillary action, in which water moves through pores due to the forces of cohesion and adhesion opposing gravity, allowing a significant amount of water to encounter solar radiation in a small area of the basin. Blackening the sponges may result in the pores becoming sealed and hinder capillary action of sponge. Due to the small size of the basin, four sponges were preferred.

Table 3
The mechanical and chemical properties, along with the size of the grey limestone used in the present study [84].

Mechanical properties		Chemical properties	
Parameter	Value	Composition	Percentage (%)
Hardness (Moh's scale)	3–4	CaO	38–42
Compressive strength (kN/m^2)	2500–2700	SiO_2	15–18
Density (Kg/m^3)	$6 \times 10^{10} - 1.7 \times 10^{11}$	Al_2O_3	3–5
Water absorption (%)	<1	MgO	0.5–3
Size (m)	0.0127	Alkalies	1–1.5
		$FeO + Fe_2O_3$	1–1.5
		Others	30–32

2.2. Preparation of the hybrid nano-PCM

The adding of nanoparticles to PCM (paraffin wax) is one of the most efficient methods for improving the material's thermal conductivity [87]. The majority of studies have concentrated on this topic since the dispersion of nanoparticles in the PCM is the key component. Most studies have employed the stirring approach to combine nano particles with the PCM. The procedures describe below can be utilized for producing (HNPCM) [87]. In the beginning, paraffin wax was melted in a beaker set over a hot plate at 80 °C to create HNPCM (Fig. 3(a)). Al_2O_3 and ZnO nanoparticles are introduced separately with weight ratios of 2 wt% and 2 wt%, once paraffin wax has completely melted. The mixture was stirred with a magnetic stirrer at 500 rpm and 80 °C for 90 min, as illustrated in Fig. 3(b), after which it was placed in a sonication machine for 2 h to achieve full particle dispersion with PCM at a medium sonication frequency as shown in Fig. 3(c). Fig. 3(d) illustrates how the hybrid nano augmented PCM was poured into the aluminum cans after two hours of sonification. Physiochemical properties of PCM, nanoparticles and HNPCM (4 wt% nanoparticles) are given in Table 4.

2.3. Experimental setup

The experimental research for the current work was conducted in September 2023 at Rajshahi University of Engineering & Technology (in the Mechanical Engineering department), Rajshahi (Longitude/Latitude: 88.6241 E / 24.3636 N). Temperature profiles, productivity, energy efficiency, and economic evaluation have been taken into consideration while evaluating and comparing the SSs' performance. The various solar still configurations used in this investigation are shown in Table 5. The experimental assessments for the current investigation are documented on an hourly basis from 9:00 a.m. to 18:00p.m. A photograph of the outdoor experimental setup is shown in Fig. 4. With the help of a TSL25911 and using high Sensitivity Digital Ambient Light Sensor, the hourly sun radiation readings were recorded. Beakers were used to gather the fresh water that had been found in the SSs. Case-I, II, III and IV are shown in Fig. 5.

3. Mathematical expression for assessing efficacy

This section provides a diverse range of numerical equations to evaluate the performance of the proposed systems. These include energy and exergy efficiency, environmental analysis, sustainability index, energy production factor (EPF), energy payback time (EPBT), exergoeconomic analysis, and uncertainty estimation. The system is presumed to function in a stable state, with consistent thermal properties such as specific heat, thermal conductivity, and latent heat. In addition, other factors such as wind velocity, and cloud coverage were not considered.

3.1. Energy analysis

Considering the ratio of the quantity of thermal energy used to produce a specific amount of distilled water to the incident solar energy during a specified time interval, the distiller unit's thermal efficiency may be characterized [88]. Eq. (1) [89], where $\dot{m}_w$ is the freshwater productivity (kg/day), is used to calculate the thermal energy efficiency of the SS on a daily basis. I_s is for solar irradiation (W/m^2), A_b for SS area

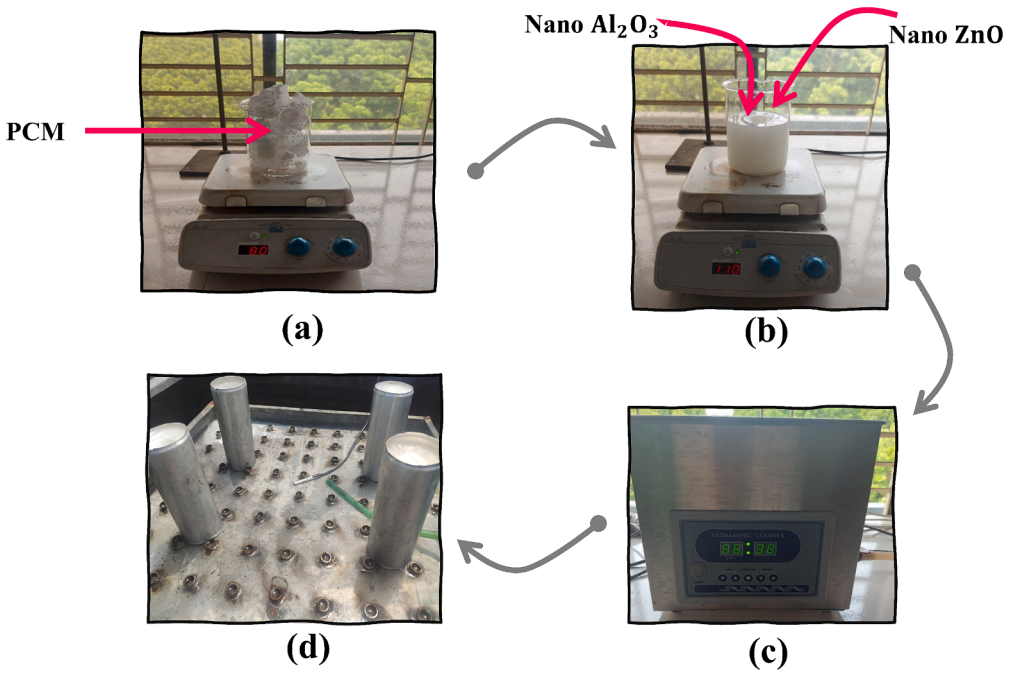

Fig. 3. Preparation of the hybrid nano-enhanced PCM by (a) melting paraffin wax in a beaker at 80 °C, (b) adding Al_2O_3 and ZnO nano-particles with equal proportion and stirred with a magnetic stirrer at 500 rpm and 80 °C for 90 min, (c) placed the melted mixture to the ultrasonic sonication machine for 2 h, (d) poured the mixture to the cylindrical aluminum cans.

Table 4
The dimensional parameters of the SS.

Material	Physiochemical properties with value
Paraffin wax (Kabeel et al., 2016)	Melting temperature (56–58 °C) Specific heat of liquid/solid (2510/2950 J/kg.°C) Thermal conductivity of 0.24/0.24 W/m.°C (liquid/solid)
Al_2O_3 (Nanoparticles) (Essa et al., 2020)	Density (3900 kg/m^3) Thermal conductivity (46 W/m.K)
ZnO (Nanoparticles) (Thakur et al., 2021)	Thermal conductivity (6.5 W/m.K) Density (6000 kg/m^3) Specific Heat (443.4 J/kg.K)
Hybrid nano-enhanced PCM	Latent heat capacity (228.93 kJ/kg) Thermal conductivity (2.18 W/m.K)

Table 5
Different configurations of Solar still.

Cases	Description
Case-I	Conventional solar still (CSS)
Case-II	Conventional solar still with fins and black sand
Case-III	Conventional solar still with fins, hybrid enhanced nano PCM, black sand and sponges
Case-IV	Conventional solar still with fins, hybrid enhanced nano PCM, crushed stone and sponges

(m^2), Δ t stands for time (Sec), and h_{fg} stands for latent heat of evaporation of water (J/kg K) that can be obtained by Eqs. (2) and (3).

$$\eta_{th} = \frac{\dot{m}_w h_{fg}}{I_s A_b \Delta t} \tag{1}$$

$$h_{fg} = 3.1615\left(10^6 - 761.6T_i\right), T_i > 343 \tag{2}$$

$$h_{fg} = 2.4935\left(10^6 - 947.79T_i + 0.13132T_i^2 - 0.0047974T_i^3\right), T_i < 343 \tag{3}$$

where, $T_i = \frac{T_1+T_3}{2}T_1$ = Basin water temperature (K).
T_3 = Inner glass cover temperature (K).

3.2. Exergy analysis

To determine how much useable energy is present in the system for a certain purpose, such as a solar still, exergy efficiency was estimated [90]. When the system enters thermodynamic equilibrium for a certain state, the exergy determines the usable work that may be accomplished from the SS. The second law of thermodynamics provides the foundation for the exergy analysis. The exergy efficiency can be given as follows [91,92]:

$$\eta_{ex} = \frac{\dot{E}_{x,out}}{\dot{E}_{x,in}} \tag{4}$$

where, The output exergy in Watt is determined from the relation [91,92],

$$\dot{E}_{x,out} = \dot{m}_w h_{fg}\left[1 - \frac{T_4}{T_1}\right] \tag{5}$$

However, the input exergy in Watt can be calculated by using the following relation [91,92],

$$\dot{E}_{x,in} = I_s A_b\left[1 - \frac{4}{3}\left(\frac{T_4}{T_s}\right) + \frac{1}{3}\left(\frac{T_4}{T_s}\right)^4\right] \tag{6}$$

where, Sun temperature,$T_s = 6000K$ [93].
T_4 = Ambient temperature (K).

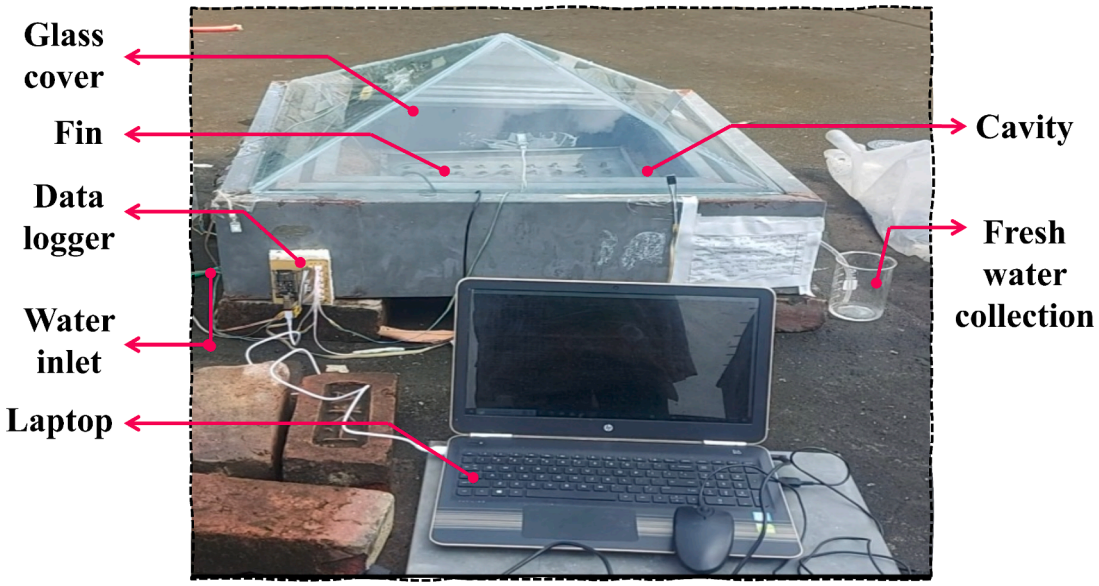

Fig. 4. Experimental setup with the attached components.

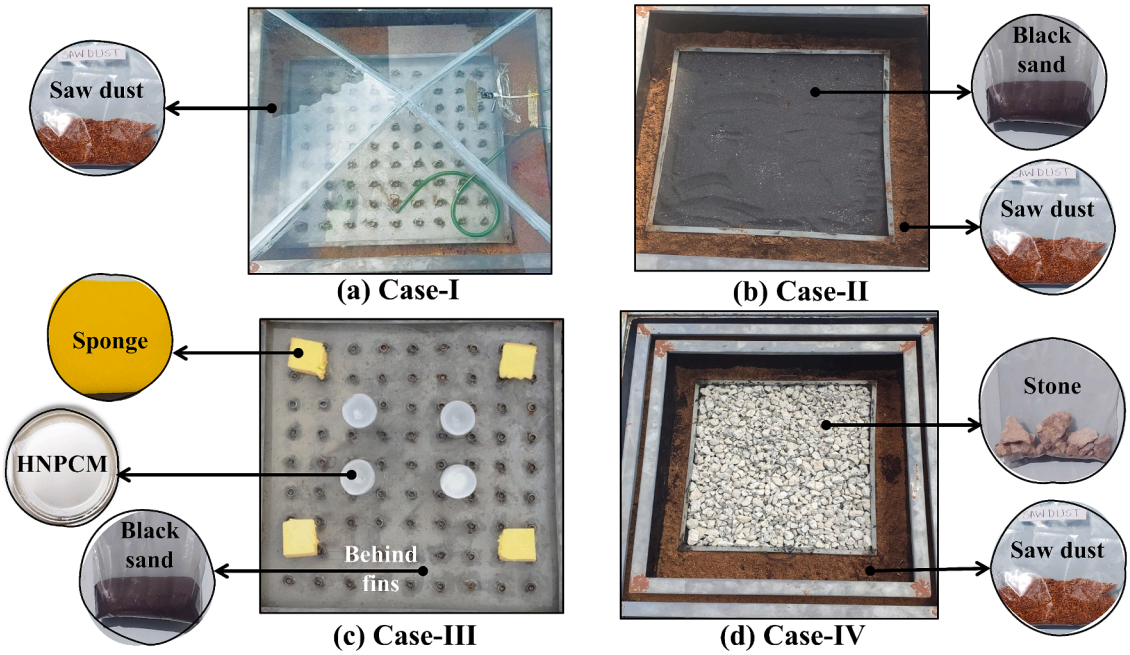

Fig. 5. Configuration for four cases.

3.3. Economic analysis

It is crucial to assess any energy system's viability from an economic perspective. Because it shows whether or not the suggested solution is lucrative and sensible from the end user's perspective. In this study, the suggested system was examined using the Uniform Annual Cost (UAC) technique [94]. The price of distillate produced by a solar desalination plant depends on a variety of parameters. The size of the unit, the location of the site, the characteristics of the feed water, the needed quality of the product water, the availability of skilled employees, etc. all affect the capital and operating expenses (and hence the overall expenditures). The primary economic benefits of solar desalination should not need extensive infrastructure because it is straightforward to construct, install, run, and maintain locally [95]. The cost of producing the distilled water and its suitability determine the investment's best return on capital.

3.3.1. Cost analysis

In the case of economic analysis, the main metric and factor is the cost per liter. Cost per liter can be obtained for four cases of modified ss by utilizing these Eqs. (7)–(14). Taking an interest rate (%) for return i and n is the considering life of solar still (years). Cost recovery factor is determined from the following relation [95],

$$CRF = \frac{i(1+i)^n}{(1+i)^n - 1} \tag{7}$$

Fixed annual cost (FAC) in dollars and sinking fund factor (SFF) can be determined from the Eqs. (8) and (9) [95],

$$FAC = P \times CRF \tag{8}$$

$$SFF = \frac{i}{[(i+1)^n - 1]} \tag{9}$$

Salvage value (S) in dollars and annual salvage value (ASV) in dollars can be calculated using Eqs. (10) and (11) [95],

$$S = 0.2 \times P \tag{10}$$

$$ASV = SFF \times S \tag{11}$$

AMC is the annual maintenance cost in dollars and TAC is the total annual cost in dollars, which can be calculated by the Eqs. (12) and (13) [95],

$$AMC = 0.15 \times FAC \tag{12}$$

$$TAC = (FAC + AMC - ASV) \tag{13}$$

The cost per liter ($/L) can be determined from the Eq. (14), where M is the mean annual production in (L/m^2) [95],

$$CPL = TAC/M \tag{14}$$

3.3.2. Payback period

The payback period is a financial metric used to determine the time it takes to recover an initial investment. Payback period is estimated from the Eqs. (16) and (17) [78]. Here, P stands for capital cost in dollars.

$$Marketpriceofdistilledwater = 0.27(\$/L \tag{15}$$

$$Gain = Avg.Yield \times marketprice(\$/m^2/day \tag{16}$$

$$Paybacktime = P/Gain(days \tag{17}$$

3.4. Environmental analysis

The environmental analysis might be used as a suitable indication to gauge how much carbon dioxide the solar distillation system has reduced. A crucial strategy has to be taken into account alongside any energy system's energetic and economic analyses. Since the suggested system must also benefit the environment. However, there are currently no markets or avenues for the sale of carbon credits generated by solar distillation systems. This method determines how much carbon dioxide is avoided if a system is powered entirely by renewable energy sources, in this instance SSs [94]. However, the resources utilized in the construction of these renewable-based systems are derived from fossil fuels, which pollute the environment. In order to evaluate the benefits and dangers of these renewable-based technologies from an environmental standpoint, it is also required to evaluate the impact of these contaminants in addition to the beneficial effects of these systems. The quantity of energy used to fabricate each element and element of the SS system is known as embodied energy [94].

3.4.1. CO_2 emission and mitigation calculation

CO_2 emission,X_{CO_2} in Kg, is calculated by following Eq. (18) [45],

$$X_{CO_2} = \mu_{CO_2} \times E_{in} \tag{18}$$

Where, μ_{CO_2} is the CO_2 emission factor for the electricity mix, which is equivalent to 0.465 kg/kWh (in Bangladesh) [96]. The embodied energy is denoted as E_{in} in kWh. CO_2 mitigation,Y_{CO_2} in ton, can be calculated by the following Eq. (19) [45].

$$Y_{CO_2} = \frac{\mu_{CO_2} \times \left[\left(En_{out,ann} \times n\right) - E_{in}\right]}{1000} \tag{19}$$

where,$En_{out,ann} = \frac{\dot{m}_w \times h_{fg}}{\Delta t}$ in kWh

3.4.2. Carbon credit gained

Carbon credit gained is calculated by using following Eq. (20) [45]. In addition, on global markets, the price of carbon currently varies from $13 to $16 per ton. As a result, experts determined that an average of $14.5 per ton of carbon was appropriate [97].

$$CCG = Y_{CO_2} \times CostofCO_2perton \tag{20}$$

3.5. Sustainability analysis

Any system that relies on renewable energy must examine its energy matrix, which may be thought of as one of the simplest and simplest decision-making instruments. Energy matrices are crucial because they show whether or not employing these renewable energy sources makes sense [94]. Because it showed a comparison between the energy used during production and the energy collected by the system over its lifetime of operation [94]. In this section, the energy production factor (EPF) and the energy payback time (EPBT) as two energy matrix criteria are calculated for the modified SS.

3.5.1. Energy payback period and energy production factor

The energy payback time (EPBT) criterion may be described using an energy and exergy method and is defined as the amount of time required to recover the embodied energy of the SS system [94]. Energy payback period and energy production factor can be calculated by the following Eqs. (21) and (22) [98],

$$EPT_{En} = \frac{E_{in}}{En_{out,ann}} \text{ in yr.} \tag{21}$$

$$EPF_{En} = \left[\frac{E_{in}}{En_{out,ann}}\right]^{-1} \text{ in } (\text{yr.})^{-1} \tag{22}$$

3.5.2. Sustainability index

The efficient functioning of a system's utilization of resources is evaluated by its sustainability index (SI). That means, it is a measure that indicates how well resources are utilized. According to the exergy efficiency, this parameter is determined as follows by Eq. (23) [99]:

$$SI = \frac{1}{1 - \eta_{EX}} \tag{23}$$

The sustainability index value ranges from 1 to ∞ and can be any positive integer [45].

3.6. Exergo-economic analysis

Exergy analysis, which gauges energy quality, and economic assessment are combined in exergo-economic analysis. This enables you to assess both the quality of the energy utilized in the process as well as how well a solar still turns solar energy into clean water. For system performance to be optimized, this is essential. Exergo-economic parameter in kWh/$ is obtained by following Eq. (24) [93],

$$R_{En} = \frac{En_{out,ann}}{TAC} \tag{24}$$

3.7. Heat transfer analysis

This part illustrates the process of heat transmission from the water to the inner glass of the SS.. The three mechanisms of heat transfer, convection, evaporation, and radiation are investigated [94] and represented in Table 6.

3.8. Total solid, total dissolved solid, and total suspended solid tests of river, discolored water, and output water samples

Total solid (TS), Total dissolved solid (TDS), and Total suspended

Table 6
Heat transfer mechanisms in several segments of SS.

Expression	Interpretation	Ref.	No. of Equation
$P_w = exp\left(25.317 - \frac{5144}{T_1 + 273}\right)$	Vapor pressure that is partially saturated at water temperature	[88]	(25)
$P_g = exp\left(25.317 - \frac{5144}{T_3 + 273}\right)$	Vapor pressure that is partially saturated at the condensing cover temperature	[88]	(26)
$h_{conv} = 0.884\left[T_1 - T_3 + \frac{(P_w - P_g)(T_1 + 273)}{268.9 \times 10^{-3} - P_w}\right]^{\frac{1}{3}}$	The ratio of convective heat transfer between glass and water	[88]	(27)
$h_{evap} = 16.273 \times 10^{-3} h_{conv} \frac{P_w - P_g}{T_1 - T_3}$	The coefficient of evaporative heat transfer between glass and water	[88]	(28)
$\varepsilon_{eff} = \left(\frac{1}{\varepsilon_w} + \frac{1}{\varepsilon_g} - 1\right)^{-1}, where \varepsilon_{eff} 0.8489$	The effective water surface emissivity to the glass cover is ε_{eff}	[88]	(29)
$h_{rad} = \varepsilon_{eff} \times \sigma \times \left[(T_1 + 273)^2 + (T_3 + 273)^2\right](T_1 + T_3 + 546)$	The coefficient of radiative heat transfer between glass and water	[100]	(30)
$h_{Total} = h_{conv} + h_{evap} + h_{rad}$	The SS's overall heat transfer coefficient	[100]	(31)

solid (TSS) tests were performed to know how much-suspended solids and total dissolved solids can be removed by modified SS. Solids in water that a filter can capture are known as TSS. In addition, TS are the suspended and settleable solids in water along with dissolved solids. TDS in water includes both volatile and non-volatile solids. River (Padma) water and discolored water were feed to the SS in case-III after performing TS, TSS and TDS test on those samples and TS, TDS, TSS test were performed on the output obtained after using river water and discolored water as feed water to highlight if output water contains any dissolved solids or not. TS, TSS and TDS tests were performed by following procedure. At first symbolized two empty beakers as T and D for each test of the sample. T was referred for the total solid test of the sample and D was referred for the total dissolved solid test of the samples. Then, two beakers were heated for 10 min to evaporate any vapors inside the beaker. Then, two empty beakers T and D were weighed, (T_{w1}, D_{w1}). After that, 100 ml sample water was taken in T symbolizing the beaker. After this, a filter paper was set in a rotating cylinder. Then, another 100 ml of water of the same sample water was allowed to pass through the filter paper. After filtration, the filtered water was poured into the D-symbolizing beaker. The filter paper separated the suspended solid from the sample water. Further, these two beakers were put on the heater and weighed (T_{w2}, D_{w2}) till the water in the two beakers completely evaporated. Then, two beakers were allowed to cool at an ambient temperature for a few minutes. After this, T and D beakers were weighed and the following calculations were made for each sample and values obtained for each sample. Total solid (TS), Total dissolved solid (TDS) and Total suspended solid (SS) can be determined using the following Eqs. (32)–(34),

$$TS = \frac{T_{w2} - T_{w1}}{100} \times 1000(g/L) \tag{32}$$

$$TDS = \frac{D_{w2} - D_{w1}}{100} \times 1000(g/L) \tag{33}$$

$$SS = TS - TDS(g/L) \tag{34}$$

3.9. Experimental uncertainty analysis

In the experimental studies, it is mandatory to ensure that the experimental outcomes are free from fault while every experiment should deal with a number of independent variables. Some of these errors are systematic related to the used equipment, made by the researcher, and for the environmental impact. Cloud cover and humidity have an impact on solar still performance. Furthermore, additional factors including wind speed, air–water vapor content, and the portion of the sky covered by clouds were not taken into account. In some cases, the causes associated with errors can be figured out and solved easily but in most of cases, the experimental results don't match with our expectations and that doesn't mean that those outcomes are meaningless. The uncertainty values of the used equipment are given in Table 7.

To determine the combined standard uncertainty, the following equation has been adopted [101]:

$$W_R = \left[\left(\frac{\partial R}{\partial x_1}\omega_1\right)^2 + \left(\frac{\partial R}{\partial x_2}\omega_2\right)^2 + \cdots + \left(\frac{\partial R}{\partial x_n}\omega_n\right)^2\right]^{1/2} \tag{35}$$

where W_R represents the total uncertainty of the equipment, R denotes the function of dependent variables, and $(\omega_1, \omega_2, \cdots\cdots, \omega_n)$ are the uncertainty in the independent variable. Additionally, the hourly productivity is the function of the basin water depth; $m = f(h)$. Hence, the combined uncertainty of the water productivity can be calculated as follows [102]:

$$W_m = \left[\left(\frac{\partial m}{\partial h_1}\omega_h\right)^2\right]^{\frac{1}{2}} \tag{36}$$

The thermal efficiency is the function of hourly productivity and the solar intensity and can be written as:

$$\eta_{th} = f(m, I(t)) \tag{37}$$

The combined uncertainty of thermal efficiency can be computed as follows [102]:

$$W_{\eta_{th}} = \left[\left(\frac{\partial \eta_{th}}{\partial m}\omega_m\right)^2 + \left(\frac{\partial \eta_{th}}{\partial I_R}\omega_{I(t)}\right)^2\right]^{\frac{1}{2}} \tag{38}$$

Considering the coverage factor (k) and confidence level (assuming 99 % for manufacturing industry), the equation of expanded uncertainty can be written as follows [103]:

$$U = kW_R \tag{39}$$

Coverage factor will be computed in the Excel by using the following function [103]:

$$k = TINV(probability, degreesoffreedom) \tag{40}$$

The probability will be estimated by using following formula [103]:

Table 7
Uncertainty values of used equipment.

Sr. No.	Instrument	Parameter	Range	Accuracy
1	Sensor (DS18B20)	Temperature	−55 °C to + 125 °C	±0.5 °C
2	Sensor (TSL25911)	Radiation	0–88000 W/m^2	±1 W/m^2
3	Flask	Water quantity	0–2000 ml	±5 ml

$$Probability = (1 - \alpha) \quad (41)$$

Where, α is the confidence level and use 1,000,000 for infinity degrees of freedom.

Accordingly, the values of errors associated with the daily water productivity and the thermal efficiency are by around ± 1.29 % and ± 4.2 % respectively by considering the coverage factor and confidence level.

4. Results and discussion

The most environmentally friendly method of turning salty saltwater into freshwater is solar desalination. Research on saltwater desalination over the last several decades has discovered a method to use various renewable energy sources to make the process more affordable and environmentally benign. The effect of solar radiation, the climate, the design criteria, the phase-change material, heat transfer, etc. all have an impact. In this section, the result obtained from the previous article are widely discussed and compared various parameter for case-II, III and IV with case-I.

4.1. Variations in temperature and their implications

For cases-I, II, III, and IV, the experimental data collected throughout the research are provided in Fig. 6(a)–(d), separately. For 8 to 9 h of measurement on a sunny day, the solar intensity varied from 30 to 680 W/m^2 with a reasonably constant ambient temperature (31 to 40 °C). Fig. 6 illustrates how the solar elements' temperature varies gradually toward its maximum value six hours afterwards sunrise before gradually decreasing by sunset. The maximum temperatures recorded in case-I were 65.78 °C for the basin water, 45.69 °C for the outer glass cover, and 52 °C for the inner glass cover surface as shown in Fig. 6(a). The maximum temperature differences between the inner glass cover surface and basin water were 18.28 °C, while those between the inner and outer glass were 6.31 °C. This indicates that the condensation process proceeded quickly as a result to the growing temperature gradient between the inner glass cover and basin water. The maximum temperatures recorded in case-II were 62.72 °C for the basin water, 46 °C for the outer glass cover surface, and 50.41 °C for the inner glass cover surface as represented in Fig. 6(b). The early absorption of solar radiation by fins and sand causes a modest reduction in the temperature increase of the basin plate compared to case-I. The absorber plate's heat was absorbed by the brackish water, which then warmed up. After 15:00 h, some of the incident energy that was absorbed by the sand was transferred to the water in the basin. Due to the fact that sand acts as a sensible heat source and releases its stored energy to the SS basin water sections later in the day, the temperature of the components in case-II is always greater than in case-I from 15:00 to 17:00 h. For case-III as shown in Fig. 6(c), the maximum temperatures measured were 62.6 °C for the basin water, 47.17 °C for the outer glass cover surface, and 50.4 °C for the inner glass cover surface. The temperature trend was discovered to be comparable to cases-I and II. In order to absorb more heat from the absorber plate and solar radiation, the HNPCM in this still boosts thermal conductivity later section of day. By introducing more conduction regions, the hollow circular fins also increase the heat transfer coefficient. The absorber plate's extremely conductive fins greatly reduce the hybrid nano-enhanced PCM's charging and discharging time. For case-IV as shown in Fig. 6(d), the highest temperatures recorded for the basin water, the

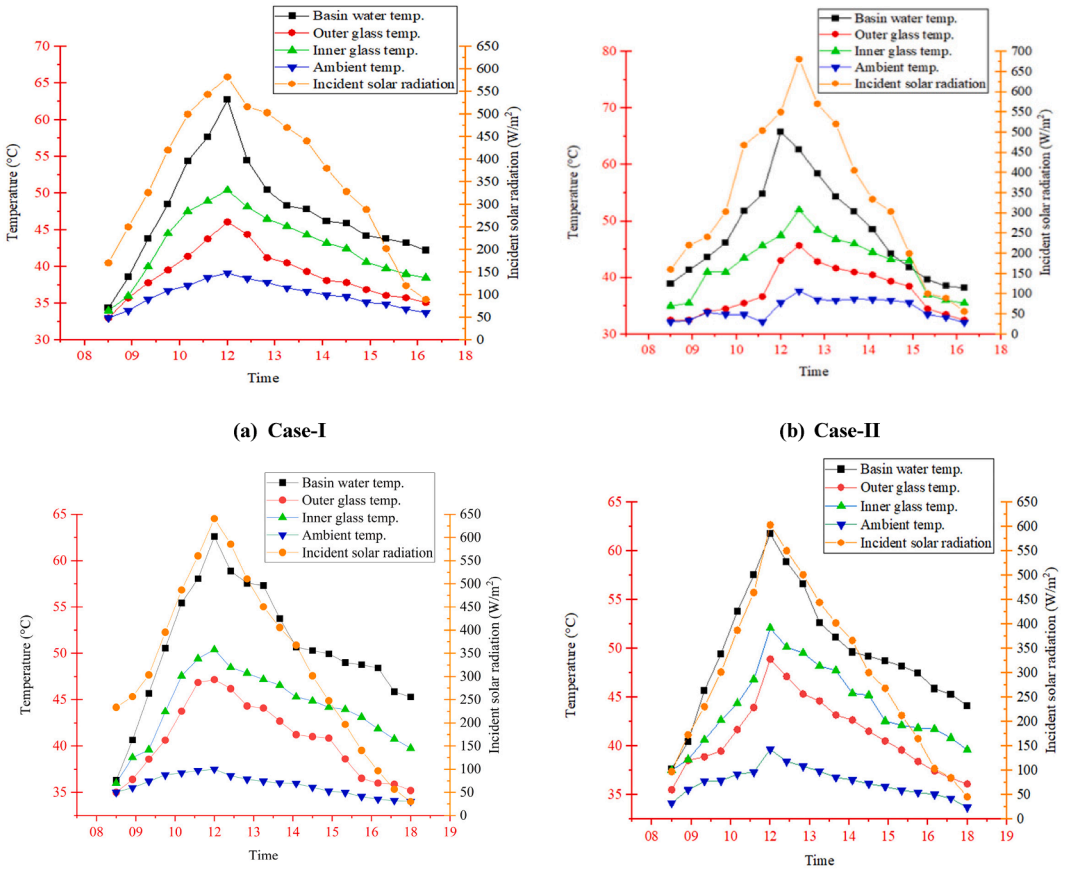

Fig. 6. Solar intensity and temperatures profile for case-I, II, III and IV.

outside glass cover surface, and the inner glass cover surface were 61.75 °C, 48.9 °C, and 52.1 °C, respectively. The trend in temperature was comparable to that seen in case-III. Additional absorption of heat from the basin plate and solar radiation had been accomplished by using the HNPCM and stones. The hollow circular fins boost the heat transfer coefficient by adding more conduction areas. Black sand served as a more sensible heat source than stone.

4.2. The effect of PCM on the basin water temperature

Due to the use of the hybrid nano-enhanced PCM, a high basin water temperatures were observed in the case-III and case-IV in compare with the case-I and case-II. About 8.17 % to 26.317 % basin temperature was increased from 15:00 hr. to 17:00 hr. in the case-III compare with the case-I due to the combined effects of HNPCM and black sand. In the case-IV compared to the case-I, the basin temperature increased by 5.83 % to 19.61 % between 15:00 and 17:00 h as a result of the combined impacts of the HNPCM and stone as shown in Fig. 7.

4.3. Productivity of modified solar still

Producing freshwater is the primary objective of a solar still. Studying the effect of system modifications on the still yield is therefore essential. The maximum overall solar still production for case-I was 1640 ml/m^2. For the case-II, the maximum daily productivity was achieved 2120 ml/m^2. In the case-III, the maximum daily productivity reached 3200 ml/m^2. The maximum daily productivity gained 2400 ml/m^2 for case-IV. The maximum productivity achieved in case-III compared to all cases. Due to its higher temperature in the basin water than the other three, case-III produces more vapor than the rest of them. As a result, in comparison to the other scenarios, the evaporation and condensation rates inside case-III increased. Therefore, the daily average productivity was increased about 33.8 % (case-II), 92.8 % (case-III) and 60 % (case-IV) compared to the conventional solar still as illustrated in Fig. 8.

4.4. Efficiency of modified solar still

Fig. 9 indicates the solar system's effectiveness throughout the day in all situations. In comparison to cases-II, III, and IV, case-I's efficiency is significantly lower. It is probably due to the poor evaporation causes smaller temperature difference from the water in the basin to the inner glass. The highest energy efficiency of solar stills in cases-I, II, III, and IV was 23.33 %, 27.365 %, 36.243 %, and 34.04 %, respectively.

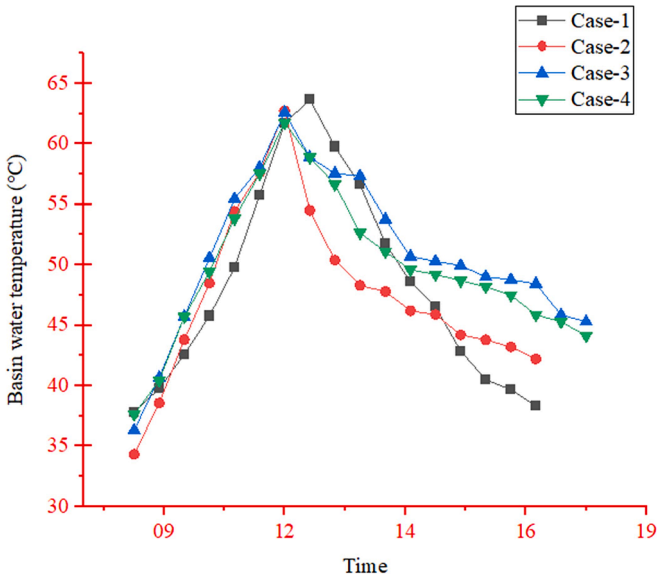

Fig. 7. Effect of HNPCM on the basin water temperature.

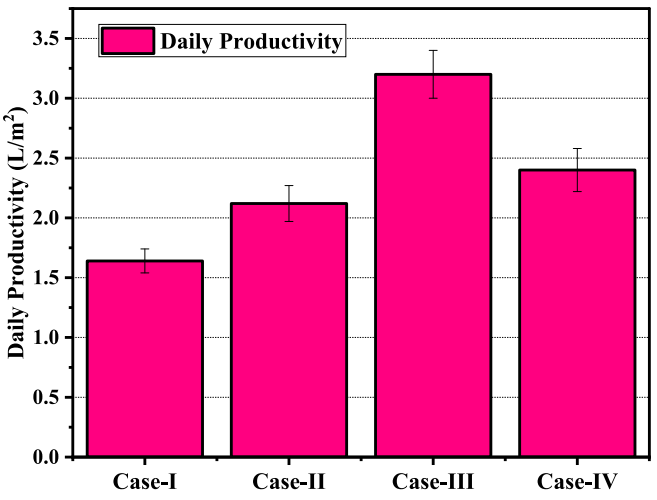

Fig. 8. Daily productivity of the modified solar still for all Cases.

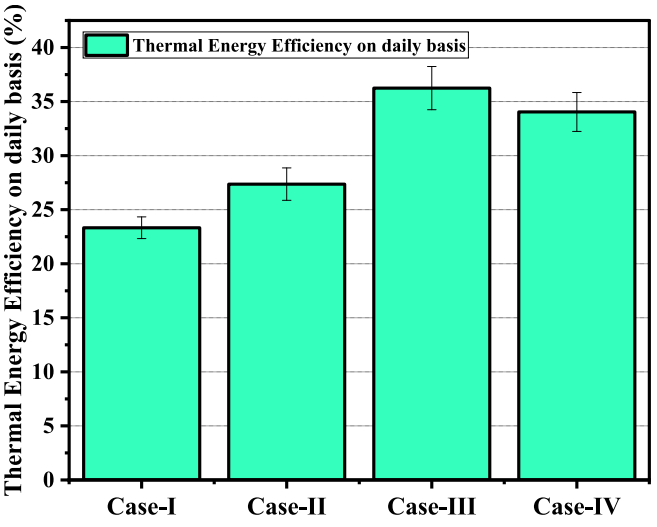

Fig. 9. Daily average thermal energy efficiency for all cases.

The maximum efficiency is found in case-III is 36.243 % due to additional energy dissipation from the HNPCM and black sand from 16:00 hr. to 18:00 hr. during the low intensity, resulting in higher evaporation due to the maintenance of high basin water temperatures during this period compared to the other cases.

As observed in Fig. 9, the daily average overall efficiency of solar still for case-II, case-III, case-IV is higher than case-I by 17.295 %, 55.35 % and 45.9 %, respectively due to the use of the latent heat storage and sensible heat storage. The daily average thermal efficiency of case-III is about 32.44 % and 6.47 % higher than case-II and case-IV due to the use of the improved latent heat storage and sensible heat storage.

4.5. Heat transfer results

From the experimental data, it has been found that the convective heat transfer co-efficient between basin water and inner glass cover surface are almost similar for all the cases during 9:00 am to 18:00 pm. The evaporative heat-transfer co-efficient (h_{evap}) between basin water and inner glass cover surface had reached peak value around 12:00p.m.

The overall heat-transfer co-efficient of modified SS had achieved to peak value around 12:00p.m. The maximum convective heat-transfer

co-efficient (h_{conv}) for case-I, II, III and IV was 2.4268 W/m^{2}K, 2.99 W/m^{2}K, 2.5638 W/m^{2}K and 2.3763 W/m^{2}K, respectively. The maximum overall heat transfer co-efficient (h_{Total}) of modified SS was 40.11 W/m^{2}K, 47.754 W/m^{2}K, 42.1728 W/m^{2}K and 40.052 W/m^{2}K, correspondingly for cases-I, II, III and IV as represented in Fig. 10(a)–(d), individually. The higher the overall heat transfer co-efficient (h_{Total}), the higher the heat transfer between basin water surface and inner side of the glass cover. Higher overall heat-transfer co-efficient (h_{Total}) results in higher evaporation of basin water. Thus, the productivity enhances around 12:00p.m.

4.6. Exergy analysis

Fig. 11 shows exergy input and exergy output for all cases. The temperature of the ambient and basin water affects the exergy. In cases-I, II, III, and IV, the maximum variance in temperature between the basin water and ambient air was 30.22 °C, 23.6 °C, 25.1 °C, and 22.1 °C, respectively.

The evaporative efficiency of the solar stills is significantly enhanced by an elevation in water temperature. Reduced ambient temperature raises the modified SS's output exergy and exergy efficiency. The output exergy and the exergy efficiency increase as the temperature of the basin rises. Input exergy decreases as ambient temperature rises, improving exergy efficiency. The solar stills' highest exergy efficiency in case-I, II, III, and IV was 0.99 %, 0.177 %, 1.73 %, and 1.52 %, respectively as represented in Fig. 12. Due to the greater temperature variation between the basin water and its surrounds, which induces fast evaporation and eventually increases the exergy production, case-III has a maximum exergy efficiency than case-I. The exergy efficiency of case-II, III, and IV, respectively, is 18.89 %, 74.75 %, and 53.54 % greater than that of case-I.

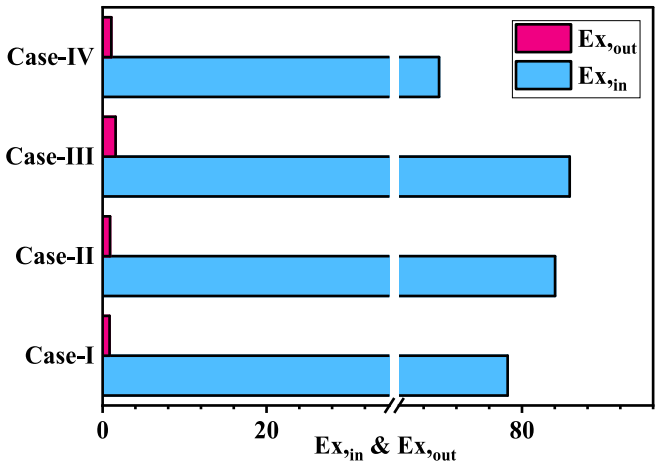

Fig. 11. Exergy input and exergy output for all cases.

4.7. Economic results

The cost per liter and payback period are the two most important variables in an economic analysis of solar stills. It aids in determining the financial viability of an investment in the modified SS.

4.7.1. Total cost and cost per liter distilled yield

In the present investigation, a cost analysis is done to examine the suggested frameworks economically. Table 8 and 9 illustrate the total cost considering 1 m^2 device area and cost per liter-distilled yield for each configuration of SS. Operating days were assumed to be 350 days per year, and the correction factor depending on Rajshahi's location

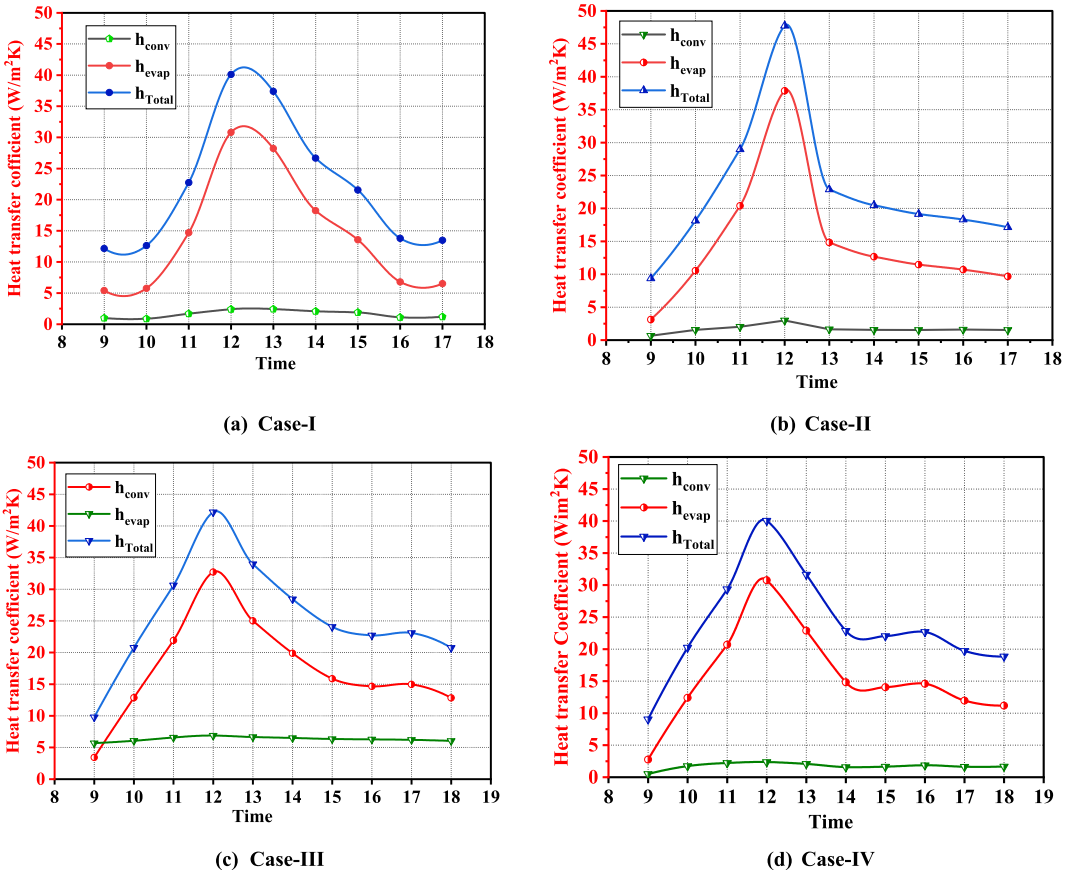

Fig. 10. Convective, evaporative and overall heat transfer co-efficient of modified SS for all cases.

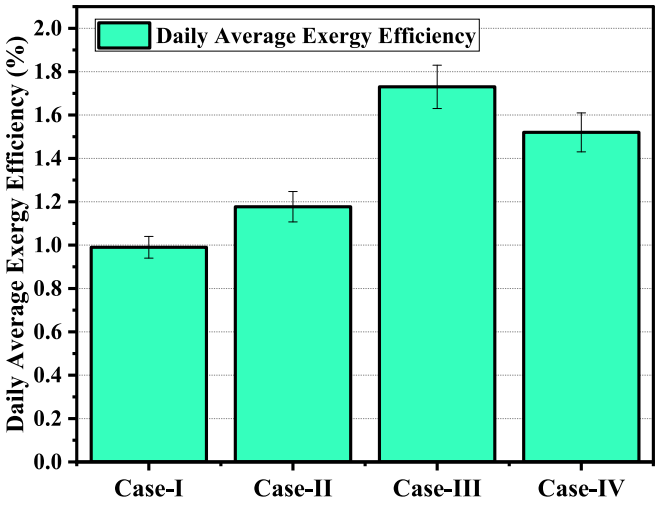

Fig. 12. Daily average exergy efficiency for all cases.

Table 8
Determination of capital cost for four cases considering 1 m^2 device area.

Cases	Material	Cost per kg ($)	Mass of the material required (kg)	Total cost ($)
Case-I	Galvanized iron sheet	4.74	10	**74.71**
	Glass cover	27.36	–	
Case-II	Galvanized iron sheet	4.74	10	**85.98**
	Glass cover	27.36	–	
	Sand	1.09	10	
Case-III	Galvanized iron sheet	4.74	10	**98.04**
	Glass cover	27.36	–	
	Sand	1.09	10	
	Al_2O_3 (Nanoparticles)	100.31	0.025	
	ZnO (Nanoparticles)	240.34	0.025	
	Sponges	0.18	1	
	PCM	2.92	1.2	
Case-IV	Galvanized iron sheet	4.74	10	**87.11**
	Glass cover	27.36	–	
	Al_2O_3 (Nanoparticles)	100.31	0.025	
	ZnO (Nanoparticles)	240.34	0.025	
	Sponges	0.18	1	
	PCM	2.92	1.2	

Table 9
Determination of cost per liter distilled yield for the four cases.

Parameters	n = 20 years, i = 10 %			
	Case-I	Case-II	Case-III	Case-IV
CRF	0.1175	0.1175	0.1175	0.1175
FAC ($)	8.7754	10.10	11.5256	10.235
SFF	0.01746	0.01746	0.01746	0.01746
S ($)	14.942	17.196	19.618	17.422
ASV ($)	0.26038	0.3002	0.3425	0.30418
AMC ($)	1.3163	1.515	1.73	1.5353
TAC ($)	9.8313	11.3148	12.912	11.466
M (L/m^2)	344.4	445.2	672	504
CPL ($)	0.0285	0.0254	0.0192	0.0228

(altitude 18 m and longitude 88.6004°) was taken as 0.6 according to Gueymard's relation [104] as follows:

$$\text{Correction factor} = \frac{0.59 \times [exp(-0.0001184 \times altitude)]^{0.5}}{Sin\,(longitude)}$$

Due to the use of the additional materials, the total cost for case-III is comparatively higher about 31.22 % than CSS.

As a result, case-III has the highest overall annualized cost. The adjustments do, however, increase productivity, which lowers the cost per liter of water produced in turn. As seen, the cost per liter for case-I is $ 0.0285, for case-II is $ 0.0254, for case-III is $ 0.0192 and for case-IV is $ 0.0228 (Fig. 13). In Bangladesh, market price of distilled water per liter is approximately $0.27. So, the reduction in cost per liter obtained from modified SS for the case-I, II, III and IV is 89.44 %, 90.59 %, 92.89 % and 91.56 %, respectively compared to the market price.

4.7.2. Payback period

The main factors in an economic study of solar stills are the cost per liter and payback period. Case-III is the most thermal energy-efficient solar still, generating more freshwater than case-I, II, and IV, according to the aforementioned study. For application and technical advancement, it must be financially feasible. The greater expense of the Al_2O_3 and ZnO nanoparticle for case-III is offset by the SS's increased productivity and quicker payback. The payback times for case-I, II, III, and IV are 185 days, 159 days, 126 days, and 135 days, respectively, as shown in Fig. 14. Therefore, case-III has a shorter payback period and is more cost-effective than other cases.

4.8. Environmental impact

Three factors—carbon dioxide emission, reduction of carbon dioxide emissions, and carbon credit gained are used to assess the environmental viability of solar stills (Table 10). The CO_2 emission and mitigation for the four distinct cases in the modified solar still are displayed in detail in Fig. 15.

Table 11 shows the embodied energy of each case. Although the components required to make solar stills, such as steel frames, glass coverings, basin plates, nano-PCM, insulation, coatings, etc., require power generated from fossil fuels during the production process, the solar stills do not emit any operating CO_2. Case-III solar still requires fins, sand nano-PCM, and hybrid nano-enhanced PCM, resulting in higher CO_2 emissions than case-I and II. The CO_2 emissions and mitigation for case-I are 73.073 kg and 358 kg. For case-II, the CO_2 emissions and mitigation are 308.79 kg and 305.4 kg. Further, CO_2 emissions and mitigation for case-III are 322.12 kg and 565 kg. Furthermore, CO_2

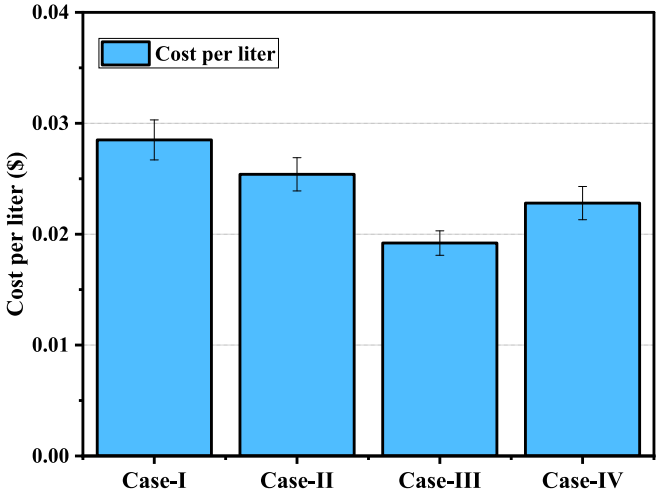

Fig. 13. Cost per liter analysis of modified SS cases.

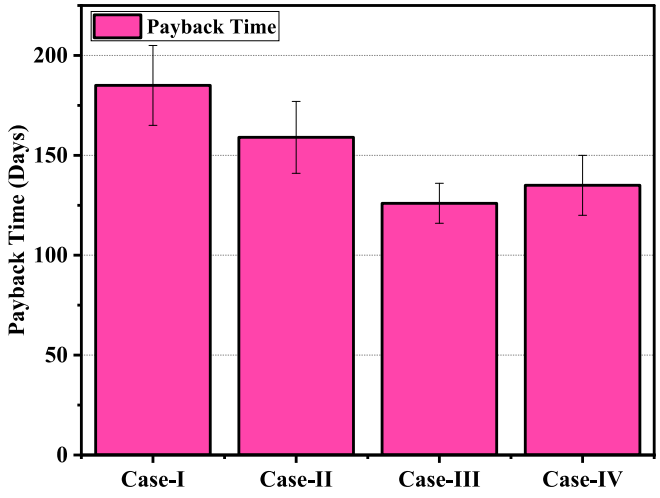

Fig. 14. Payback time for modified solar still at different cases.

Table 10
CO_2 emission, mitigation and carbon credit gained.

Cases (Consider minimum output)	E_{in} (kWh)	$En_{out,ann}$ (kWh)	X_{CO_2} (kg)	Y_{CO_2} (ton)	CCG ($)
Case-I	167.147	46.355	73.073	0.358	5.191
Case-II	664.08	66.046	308.79	0.3045	4.4283
Case-III	692.736	95.37	322.12	0.565	8.1925
Case-IV	623.296	83.9	285.18	0.4952	7.1804

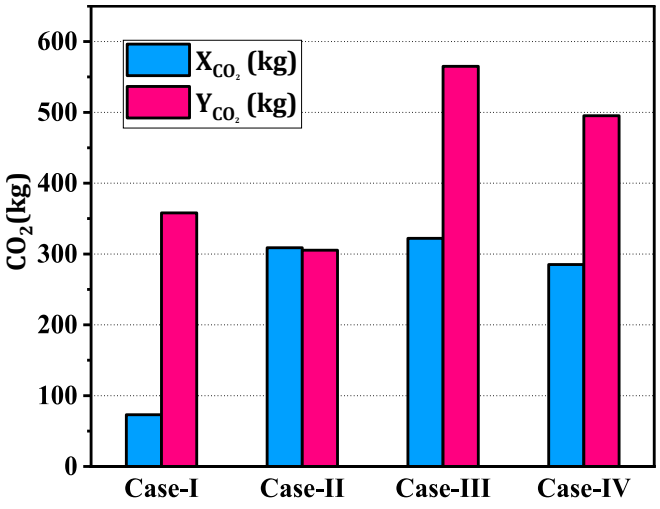

Fig. 15. CO_2 emission and mitigation for all cases.

emissions and mitigation for case-IV are 285.18 kg and 495.2 kg. Earning a carbon credit is closely correlated to the solar still's yearly energy output and CO_2 reduction. The case-III solar still offers a potential CCG of $8.1925, which is $ 1.01, $ 3.76, and $ 3 more than the case-IV, case-II, and case-I as shown in Fig. 16.

4.9. Sustainability analysis

The current study assesses the SS cases sustainability in regard to their annual production and a few pre-existing sustainability measures. The annual output amount of energy and exergy as well as the embodied energy content of the SS determines the variance in the annual production factor and payback time (Table 12). To demonstrate the sustainability of improved SS for various scenarios, three metrics are measured: the energy production factor, the energy payback duration, and the sustainability index.

4.9.1. Energy payback time

Any sustainable energy system, like as a solar still, must have its energy payback time evaluated in order to be thoroughly examined from both an economic and energy perspective. The solar still's EPT specifies how long it will take to recover the embodied energy, which is determined by how much energy was used to prepare and fabricate the parts that comprise the system. Specifically, it should be emphasized that every efficient solar still system should have more energy evolved over the course of its lifetime than originally embodied during manufacturing. The Energy Payback Time is the length of time it takes for a system of energy to produce as much energy as it consumed to construct the system. The lower the energy payback period, the faster the system will return the embodied energy of the whole system. For the case-I, the embodied energy is lowest due to the less component and has lower energy payback period. As the Fig. 17, case-III has highest embodied energy but it is compensated by high annual production due to the improvement obtain by HNPCM and black sand. For the case-I, II, III and IV energy payback period are 3.39 yr., 10.055 yr., 7.26 yr. and 7.3 yr. respectively. The EPT value for the conventional solar still tends to be lower than the EPT value for the other solar still scenarios. This is a consequence of incorporating change, which elevates the embodied energy.

4.9.2. Energy production factor

The higher the energy production factor, the more efficient evaporation which lead to the faster production of clean water. It is significant because it directly affects the performance of the distillation process. As shown in Fig. 18, energy production factor for case-I, II, III and IV are 0.295 $yr.^{-1}$, 0.099 $yr.^{-1}$, 0.138 $yr.^{-1}$ and 0.137 $yr.^{-1}$, respectively.

4.9.3. Sustainability index

A sustainability index in the context of a solar still refers to a measure of how efficiently and environmentally friendly the solar still operates. The higher the exergy efficiency, the higher the sustainability index (Table 13). A higher sustainability index is desired for more efficient utilization of resources by the system. From (Eq. (9), sustainability index for case-I, II, III and IV are 1.0099, 1.0119, 1.017 and 1.0154, respectively as shown in Fig. 19. This is due to the higher exergy efficiency is gained from the case-III in comparison to the other cases.

4.10. Exergo-economic parameter

To evaluate the link between solar still's commercial viability and energy efficiency, energy and economic assessments are combined. This integration helps to answer questions such as whether investing in more efficient material would lead to more cost-effective system over its life time. As from the Fig. 20, case-III has higher exergo-economic parameter (R_{En}) which is 7.3865 kWh/$, in comparison with case-I, II and IV. This is due to the higher energy output from the case-III in comparison to the other cases.

4.11. Total solid (TS), total dissolved solid (TDS), and total suspended solid (SS) tests results for samples

The total suspended solid obtained in filter papers after passing river water, discolored water and output water from modified SS through the filter papers are illustrated in Fig. 21. After TS tests on river water, discolored water and output water from modified SS, are shown in Table 14.

Total solid for river water is 0.4 g/L, for discolored water is 0.3 g/L and for output water from modified SS is 0.1 g/L. After TDS tests on river water, discolored water and output water from modified SS, it has been

Table 11
Embodied energy of each case.

Component	Material	Energy density		Mass (kg)	Cases			
		MJ	kWh/kg		Case-I	Case-II	Case-III	Case-IV
Body and basin [105]	Galvanized iron	50	13.88	8.5	117.98	117.98	117.98	117.98
Sand holder [105]	Galvanized iron	50	13.88	1.5	–	20.82	20.82	20.82
Basin coating [105]	Black paint	90	25	0.5	12.5	12.5	12.5	12.5
Hollow circular fins [105]	Galvanized iron	50	13.88	2.025	28.107	28.107	28.107	28.107
PCM (Paraffin wax) [105]	Paraffin wax	42	11.67	1.2	–	–	14.004	14.004
Al_2O_3 [105]	Nano-materials	200	55.56	0.025	–	–	1.389	1.389
ZnO [106]	Nano-materials	–	0.0037	0.025	–	–	0.00925	0.00925
Empty can [107]	Aluminum alloy	190–230	58.33	0.056	–	–	3.266	3.266
PVC pipe	PVC	77.90	21.40	0.4	8.56	8.56	8.56	8.56
Sand [108]	Black sand	175	48.61	10	–	486.11	486.11	–
Stone [108]	–	500	138.89	1.5	–	–	–	416.67
Total embodied energy (kWh)	–	–	–	–	**167.147**	**664.08**	**692.736**	**623.296**

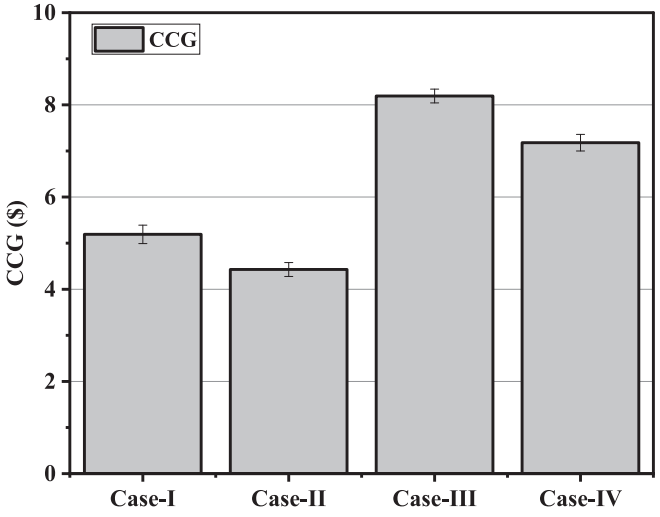

Fig. 16. Enviro-economic analysis in terms of carbon credit gained.

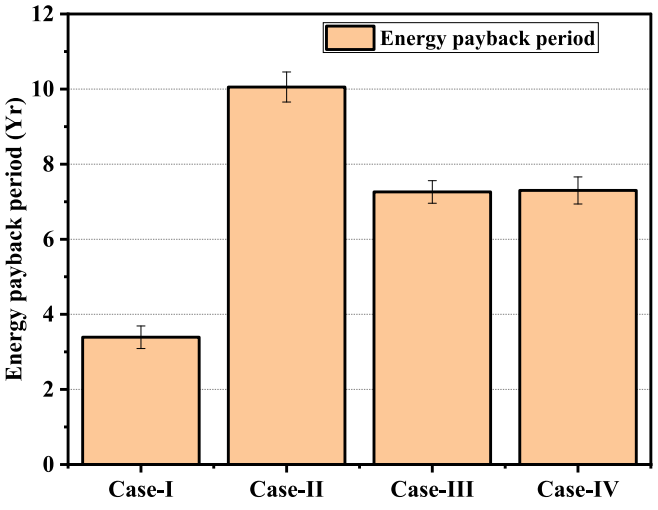

Fig. 17. Energy payback period for modified solar still.

Table 12
Determination of EPT_{En} and EPF_{En} for four cases.

Cases	EPT_{En}(yr.)	$EPF_{En}(yr.)^{-1}$
Case-I	3.39	0.295
Case-II	10.055	0.099
Case-III	7.26	0.138
Case-IV	7.3	0.137

determined that total dissolved solid for river water is 0.1 g/L, for discolored water is 0.15 g/L and for output water from modified SS is 0.1 g/L. After TSS tests on river water, discolored water and output water from modified SS, it has been computed that total suspended solid for river water is 0.3 g/L, for discolored water is 0.15 g/L and for output water from modified SS is 0.0 g/L. Therefore, no suspended solid is found in output water from modified SS in case-III.

4.12. Comparison with previous works

Conventional solar stills with fins, hybrid-enhanced nano PCM, sand, and sponges (case-III) is compared to various solar stills from earlier research in terms of three main performance parameters: daily thermal efficiency, exercise efficiency, and cost per liter. Table 15 compares the current SS to prior comparable studies.

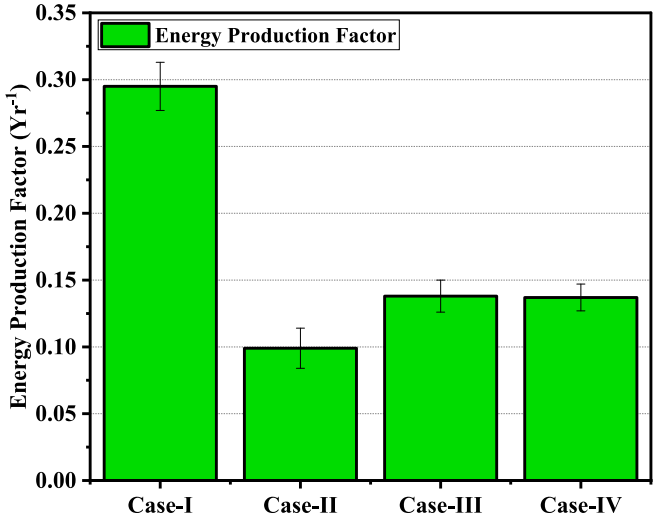

Fig. 18. Energy production factor analysis.

5. Conclusions

This study investigates a number of aspects in an effort to increase the production of SS. Improving freshwater production, performance rates, and yields are the main objectives of this investigation and highlights the effects of using hybrid nano-enhanced PCM. The research's

Table 13
Sustainability index determination for four cases.

Cases	η_{EX}(%)	SI
Case-I	0.99	1.0099
Case-II	1.177	1.0119
Case-III	1.73	1.017
Case-IV	1.52	1.0154

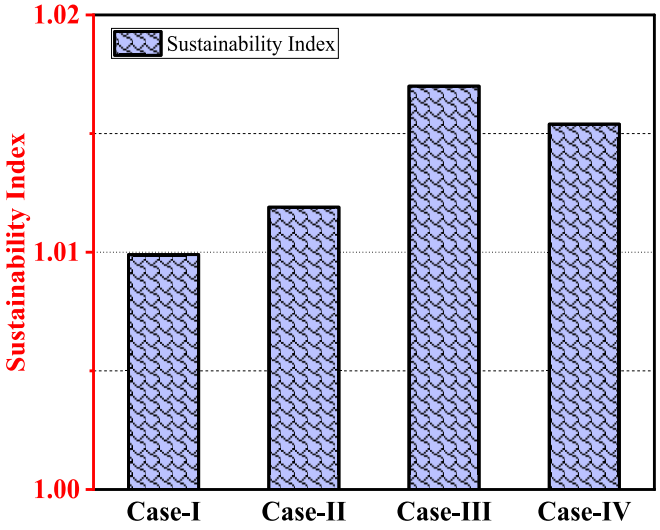

Fig. 19. Sustainability index analysis.

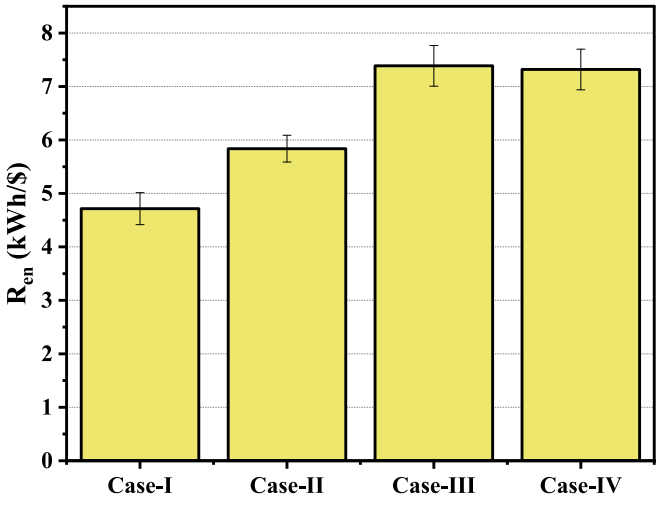

Fig. 20. Exergo-economic analysis.

key conclusions are revealed as follows:

- Due to the combined impacts of the HNPCM and black sand, the basin temperature increased from 15:00 to 17:00 h in the case-III compared to the case-I by about 8.17 % to 26.317 %. The combined effects of the HNPCM and stone increased the basin temperature by 5.83 % to 19.61 % between 15:00 and 17:00 h in case-III compared to case-I.
- When compared to all other cases, case-III's production was at its highest. When compared to the conventional solar still, the daily average production improved by around 33.8 % (case-II), 92.8 % (case-III), and 60 % (case-IV).

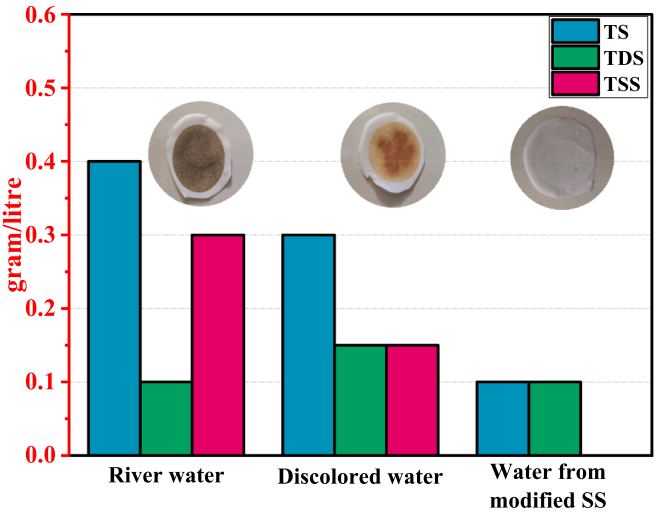

Fig. 21. Total suspended solid obtained from river water, discolored water and output water from modified SS.

Table 14
Data from TS, TDS and TSS tests.

Sample water	T_{w1}(g)	T_{w2}(g)	D_{w1}(g)	D_{w2}(g)	TS (g/L)	TDS (g/L)	TSS (g/L)
River (Padma)	111.05	111.09	112.22	112.23	0.4	0.1	0.3
Discolored water	112.83	112.86	68.94	69.09	0.3	0.15	0.15
Output water	111.05	111.06	112.15	112.16	0.1	0.1	0

Table 15
Comparison the current SS to prior comparable studies.

SS arrangement	Parameters		
	Daily thermal efficiency (%)	Exergy efficiency (%)	Cost per liter ($/L)
Pyramid solar still with corrugated absorber plate [109].	45.25–45.80	–	0.53
Tubular solar still with U-corrugated basin (basin water depth 1 cm) [110].	66.6	4.74	0.00511
Single slope with Thermoelectric generator (TEG) – iron scraps [111].	–	–	0.074
Single slope with Gravel coarse aggregate sensible heat storage [112].	–	–	0.0618
Single Slope SS with CuO nano-PCM [113].	43.02	–	0.13
Double slope SS with ISR, HCF, and Al2O3 nano-PCM [45].	22	1.8	0.0199
Present study: Case-III	36.243	1.73	0.0192

- Due to the utilization of increased latent heat storage and sensible heat storage, case-III has a daily average thermal efficiency that is about 32.44 % and 6.47 % greater than case-II and case-IV.
- CSS and case-II, II, and IV had maximum overall heat transfer coefficients (h_{Total}) of 40.11, 47.754, 42.1728, and 40.052 W/m^2 K, respectively. The heat transmission between the water surface of the basin and the inner side of the glass cover is inversely proportional to the overall heat transfer coefficient (h_{Total}). The basin water

evaporates more quickly when the total heat transfer coefficient (h_{Total}) is larger. As a result, productivity increases around 12p.m. in all cases due to high value of h_{Total}.

- In comparison to case-I, case-II, III, and IV all had exergy efficiency improvements of 18.89 %, 74.75 %, and 53.54 %, correspondingly.
- In cases-I, II, III, and IV modified SS results in cost per liter reductions of 89.44 %, 90.59 %, 92.89 % and 91.56 %, correspondingly, as compared to market prices for 350 operating days thought out the year.
- The greater the energy production factor, evaporation is more efficient and produces clean water more quickly. Cases-I, II, III, and IV's energy production factors are 0.137 yr^{-1}, 0.099 yr^{-1}, 0.138 yr^{-1}, and 0.195 yr^{-1}, respectively. Consequently, case-III is more sustainable than other cases.
- After performing TS, TDS, and TSS tests on the output water sample, there are no suspended solids to be discovered in the output water from the modified SS in case-III.

Flushing the basin with fresh water is the most straightforward method to clean up the salt deposit. By simply filling the basin with water and then emptying it, this may be accomplished. Salt deposits can be removed using a power washer if the basin is big and easily accessible. It is not advisable to apply excessive pressure since this could lead to damage the basin. Scrubbing the interior of the bowl using a brush with strong bristles. This may aid in removing salt buildup that is sticking to the surface. Gently wipe off the salt granules from the basin's surface with a scraper or spatula. It is important to proceed cautiously so as not to damage the material of the basin in the process.

6. Limitation of the study

The purpose of this study is to estimate the performance of a modified pyramid solar distillation system with the suggested improvements using a relatively small model. Building a large-scale version of the suggested system could result in a different performance in terms of systematic functionality and environmental effects.

7. Future work

- Although a lot of study has been done on certain SS parameters, relatively few studies have looked at all of the parameters at once. Fins, sponges, sand, stones and HNPCM are used in combination to advance the performance of SSs.
- With the particular emphasis on the desalination process during regular working hours, the study was carried out inside the operating hours of the laboratory or facility where the tests were being done. The time period that allowed researchers to carefully monitor and examine data is exactly the researchers have decided to concentrate on. There is still an opportunity that may be leveraged acquire data and evaluate throughout the entire day.
- Hybrid nano-particles are further included in copper balls to improve surface area and quicken heat transfer. Additionally, sponges are encouraged for increasing production rate.
- The largest improvement in energy and exergy efficiency in solar stills can be achieved with nano-fluid.
- Within the SS, black sand is also used as a sensible heat-storage element and in a variety of fin characteristics that help with the PCM's superior melting and solidification.
- More investigation is required into the filtration of produced water from SS and the purification of water for acceptable drinking. The layout of SS has been altered to ensure that the fouling factor caused by salt deposition will not affect its effectiveness.

CRediT authorship contribution statement

Usma Atiua Anika: Conceptualization, Data curation, Investigation, Methodology, Writing – original draft. **Md. Golam Kibria:** Conceptualization, Formal analysis, Supervision, Writing – review & editing. **Shithi Dey Kanka:** Data curation, Methodology, Writing – original draft, Writing – review & editing. **Md. Shahriar Mohtasim:** Formal analysis, Visualization, Writing – review & editing. **Utpol K. Paul:** Formal analysis, Writing – review & editing, Validation. **Barun K. Das:** Formal analysis, Writing – review & editing.

Declaration of Competing Interest

The authors declare that they have no known competing financial interests or personal relationships that could have appeared to influence the work reported in this paper.

References

[1] A. Kandeal, et al., Performance enhancement of modified solar distillers using synthetic nanocomposites, reflectors, cover cooling, and ultrasonic foggers: Experimental approach. Sol. Energy 254 (2023) 123–136.
[2] S.D. Kanka, et al., Impact of various environmental parameters and production enhancement techniques on direct solar still: a review, Sol. Energy 267 (2024) 112216.
[3] H. Panchal, R. Sathyamurthy, Experimental analysis of single-basin solar still with porous fins, Int. J. Ambient Energy 41 (5) (2020) 563–569.
[4] H. Panchal, I. Mohan, Various methods applied to solar still for enhancement of distillate output, Desalination 415 (2017) 76–89.
[5] H.N. Panchal, S. Patel, An extensive review on different design and climatic parameters to increase distillate output of solar still, Renewable Sustainable Energy Rev. 69 (2017) 750–758.
[6] H. Panchal, N. Patel, H. Thakkar, Various techniques for improvement in distillate output from active solar still: a review, Int. J. Ambient Energy 38 (2) (2017) 209–222.
[7] H. Panchal, et al., Experimental and water quality analysis of solar stills with vertical and inclined fins, Groundw. Sustain. Dev. 11 (2020) 100410.
[8] M.J.R. Asadabadi, M. Sheikholeslami, Impact of utilizing hollow copper circular fins and glass wool insulation on the performance enhancement of pyramid solar still unit: an experimental approach. Sol. Energy 241 (2022) 564–575.
[9] A.A. Lisboa, R. Segurado, M.A. Mendes, Solar still performance for small-scale and low-cost seawater desalination: model-based analysis and water yield enhancement techniques. Sol. Energy 238 (2022) 341–362.
[10] K.S. Dhasan, et al., Performance analysis on single slope solar still with absorber coated using iron oxide nanoparticles at different water thickness. Sol. Energy 264 (2023) 112083.
[11] F.A. Hammad, S. Shalaby, M.E. Zayed, Innovative design of a dome-shaped solar distiller enhanced with a multi-tray conical absorber basin and fountain feeding supply: experimental study with energy, exergy, and enviro-economic analyses. Sol. Energy 266 (2023) 112183.
[12] K. Modi, P. Patel, S. Patel, Applicability of mono-nanofluid and hybrid-nanofluid as a technique to improve the performance of solar still: a critical review, J. Clean. Prod. (2023) 135875.
[13] S. Tuly, et al., Effects of design and operational parameters on the performance of a solar distillation system: a comprehensive review, Groundw. Sustain. Dev. 14 (2021) 100599.
[14] S. Tuly, et al., Investigating the energetic, exergetic, and sustainability aspects of a solar still integrating fins, wick, phase change materials, and external condenser, J. Storage Mater. 55 (2022) 105462.
[15] I. Al-Hayeka, O.O. Badran, The effect of using different designs of solar stills on water distillation, Desalination 169 (2) (2004) 121–127.
[16] Frick, G. and J. Hirschmann, Theory and experience with solar stills in Chile. Solar Energy. **14**(4): p. 405-413.
[17] H.N. Panchal, P. Sanjay, Comparative analysis of indoor and outdoor tests on solar still, Desalin. Water Treat. 63 (2017) 1–5.
[18] H. Thakkar, et al., A detailed review on solar desalination techniques, Int. J. Ambient Energy 41 (9) (2020) 1066–1087.
[19] H. Panchal, et al., Annual performance analysis of adding different nanofluids in stepped solar still, J. Therm. Anal. Calorim. 138 (2019) 3175–3182.
[20] H. Panchal, Annual performance analysis of various energy storage materials in the upper basin of a double-basin solar still with vacuum tubes, Int. J. Ambient Energy 41 (4) (2020) 435–451.
[21] H. Panchal, et al., Various techniques to enhance distillate output of tubular solar still: a review, Groundw. Sustain. Dev. 9 (2019) 100268.
[22] D. Mevada, et al., Effect of fin configuration parameters on performance of solar still: a review, Groundw. Sustain. Dev. 10 (2020) 100289.
[23] A. Shyora, K. Patel, H. Panchal, Comparative analysis of stepped and single basin solar still in climate conditions of Gandhinagar Gujarat during winter, Int. J. Ambient Energy 42 (14) (2021) 1649–1659.
[24] M. Patel, C. Patel, H. Panchal, Performance analysis of conventional triple basin solar still with evacuated heat pipes, corrugated sheets and storage materials, Groundw. Sustain. Dev. 11 (2020) 100387.

[25] S.W. Sharshir, et al., A mini review of techniques used to improve the tubular solar still performance for solar water desalination, Process Saf. Environ. Prot. 124 (2019) 204–212.
[26] A.M. Manokar, et al., Comparative study of an inclined solar panel basin solar still in passive and active mode, Sol. Energy 169 (2018) 206–216.
[27] V.K. Chauhan, S.K. Shukla, Performance analysis of Prism shaped solar still using Black phosphorus quantum dot material and Lauric acid in composite climate: an experimental investigation. Sol. Energy 253 (2023) 85–99.
[28] P.V. Kumar, et al., Solar stills system design: a review, J Renewable Sustainable Energy Rev. 51 (2015) 153–181.
[29] R. Sathyamurthy, et al., Factors affecting the performance of triangular pyramid solar still. Desalination 344 (2014) 383–390.
[30] S. Yadav, K. Sudhakar, Different domestic designs of solar stills: a review, J Renewable Sustainable Energy Rev. 47 (2015) 718–731.
[31] K.A. Hammoodi, et al., A detailed review of the factors impacting pyramid type solar still performance. Alex. Eng. J. 66 (2023) 123–154.
[32] Rababa'h, H.M.J.E.c. and Management, Experimental study of a solar still with sponge cubes in basin. Energy Conversion and Management, 2003. **44**(9): p. 1411-1418.
[33] V.K. Chauhan, et al., A comprehensive review of direct solar desalination techniques and its advancements. J. Clean. Prod. 284 (2021) 124719.
[34] H.E. Fath, S. Elsherbiny, A. Ghazy, A naturally circulated humidifying/dehumidifying solar still with a built-in passive condenser. Desalination 169 (2) (2004) 129–149.
[35] A.K. Tiwari, G. Tiwari, Effect of water depths on heat and mass transfer in a passive solar still: in summer climatic condition. Desalination 195 (1–3) (2006) 78–94.
[36] R. Sathyamurthy, et al., Experimental study on enhancing the yield from stepped solar still coated using fumed silica nanoparticle in black paint. Mater. Lett. 272 (2020) 127873.
[37] S. Sharshir, et al., Enhancing the solar still performance using nanofluids and glass cover cooling: experimental study, Appl. Therm. Eng. 113 (2017) 684–693.
[38] A. Abdullah, et al., Enhancing the solar still performance using reflectors and sliding-wick belt. Sol. Energy 214 (2021) 268–279.
[39] G.F.L. Al-Doori, et al., Enhanced productivity of double-slope solar still using local rocks, Int. J. Smart Grid Clean Energy 8 (3) (2019) 307–312.
[40] Madhu, B., et al., Improving Performance of Hemispherical Solar Distillation Unit Using Paraffin Wax Encapsulated in Waste Aluminium-Cans. SSRN Product & Services.
[41] H. Tanaka, Y.J.D. Nakatake, Theoretical analysis of a basin type solar still with internal and external reflectors, Desalination 197 (1–3) (2006) 205–216.
[42] A.M. Abdulateef, et al., Optimal fin parameters used for enhancing the melting and solidification of phase-change material in a heat exchanger unite, Case Stud. in Therm. Eng. 14 (2019) 100487.
[43] A. Kabeel, et al., Performance enhancement of pyramid-shaped solar stills using hollow circular fins and phase change materials, J. Storage Mater. 31 (2020) 101610.
[44] H. Panchal, et al., Annual performance analysis of adding different nanofluids in stepped solar still, J. Therm. Anal. Calorim. 138 (5) (2019) 3175–3182.
[45] S. Tuly, et al., Investigation of a modified double slope solar still integrated with nanoparticle-mixed phase change materials: energy, exergy, exergo-economic, environmental, and sustainability analyses, Case Stud. Therm. Eng. 37 (2022) 102256.
[46] A.M. Manokar, et al., Sustainable fresh water and power production by integrating PV panel in inclined solar still, J. Clean. Prod. 172 (2018) 2711–2719.
[47] K. Rabhi, et al., Experimental performance analysis of a modified single-basin single-slope solar still with pin fins absorber and condenser, Desalination 416 (2017) 86–93.
[48] Z. Omara, A. Kabeel, F. Essa, Effect of using nanofluids and providing vacuum on the yield of corrugated wick solar still, Energy Convers. Manage. 103 (2015) 965–972.
[49] A. El-Sebaii, M. El-Naggar, Year round performance and cost analysis of a finned single basin solar still, Appl. Therm. Eng. 110 (2017) 787–794.
[50] A. El-Sebaii, et al., Effect of fin configuration parameters on single basin solar still performance, Desalination 365 (2015) 15–24.
[51] A.M. Manokar, D.P. Winston, Experimental analysis of single basin single slope finned acrylic solar still, Mater. Today:. Proc. 4 (8) (2017) 7234–7239.
[52] H.K. Jani, K.V. Modi, Experimental performance evaluation of single basin dual slope solar still with circular and square cross-sectional hollow fins, Sol. Energy 179 (2019) 186–194.
[53] V. Velmurugan, et al., Single basin solar still with fin for enhancing productivity, Energy Convers. Manage. 49 (10) (2008) 2602–2608.
[54] M.E.H. Attia, et al., A comparative study of hemispherical solar stills with various modifications to obtain modified and inexpensive still models, Environ. Sci. Pollut. Res. 28 (39) (2021) 55667–55677.
[55] S.W. Sharshir, et al., Thermo-economic performance improvement of hemispherical solar still using wick material with V-corrugated basin and two different energy storage materials, Sol. Energy 249 (2023) 336–352.
[56] E.M.S. El-Said, et al., An experimental study on carbon-metal composite tablets as solar absorbers for water distiller performance improvement, J. Clean. Prod. 414 (2023) 137431.
[57] S.W. Sharshir, et al., Thermoenviroeconomic performance augmentation of solar desalination unit integrated with wick, nanofluid, and different nano-based energy storage materials, Sol. Energy 262 (2023) 111896.
[58] K. Elmaadawy, et al., Performance improvement of double slope solar still via combinations of low cost materials integrated with glass cooling, Desalination 500 (2021) 114856.
[59] K.H. Nayi, K.V. Modi, Pyramid solar still: a comprehensive review, Renewable Sustainable Energy Rev. 81 (2018) 136–148.
[60] K.V. Modi, K.H. Nayi, S.S. Sharma, Influence of water mass on the performance of spherical basin solar still integrated with parabolic reflector, Groundw. Sustain. Dev. 10 (2020) 100299.
[61] F. Essa, et al., Experimental investigation of convex tubular solar still performance using wick and nanocomposites, Case Stud. Therm. Eng. 27 (2021) 101368.
[62] S.W. Sharshir, et al., Improving the performance of tubular solar still integrated with drilled carbonized wood and carbon black thin film evaporation, Sol. Energy 233 (2022) 504–514.
[63] A. Kabeel, Z. Omara, M. Younes, Techniques used to improve the performance of the stepped solar still—a review, Renewable Sustainable Energy Rev. 46 (2015) 178–188.
[64] F. Essa, et al., Experimental study on the performance of trays solar still with cracks and reflectors, Appl. Therm. Eng. 188 (2021) 116652.
[65] A. Kabeel, M. Abdelgaied, Enhancement of pyramid-shaped solar stills performance using a high thermal conductivity absorber plate and cooling the glass cover, Renew. Energy 146 (2020) 769–775.
[66] S. Rashidi, et al., Enhancement of solar still by reticular porous media: experimental investigation with exergy and economic analysis, Appl. Therm. Eng. 130 (2018) 1341–1348.
[67] M. Younes, et al., Half barrel and corrugated wick solar stills–Comprehensive study, J. Storage Mater. 42 (2021) 103117.
[68] M. Jobrane, et al., Theoretical and experimental investigation on a novel design of wick type solar still for sustainable freshwater production, Appl. Therm. Eng. 200 (2022) 117648.
[69] M. Elashmawy, An experimental investigation of a parabolic concentrator solar tracking system integrated with a tubular solar still, Desalination 411 (2017) 1–8.
[70] O. Maliani, et al., Investigation on novel design of solar still coupled with two axis solar tracking system, Appl. Therm. Eng. 172 (2020) 115144.
[71] I. Altarawneh, et al., Experimental and numerical performance analysis and optimization of single slope, double slope and pyramidal shaped solar stills, Desalination 423 (2017) 124–134.
[72] A. Kabeel, et al., Improving performance of tubular solar still by controlling the water depth and cover cooling, J. Clean. Prod. 233 (2019) 848–856.
[73] N.M. Shatar, et al., Energy, exergy, economic, environmental analysis for solar still using partially coated condensing cover with thermoelectric cover cooling. J. Clean. Prod. 387 (2023) 135833.
[74] E.M. El-Said, et al., An experimental study on carbon-metal composite tablets as solar absorbers for water distiller performance improvement. J. Clean. Prod. 414 (2023) 137431.
[75] P.G. Kumar, et al., Energy, exergy, economic and environmental evaluation of solar desalination system comprising different enhanced surface absorber plates. Desalination 565 (2023) 116842.
[76] E. Banoqitah, et al., Enhancement and prediction of a stepped solar still productivity integrated with paraffin wax enriched with nano-additives. Case Studies, Therm. Eng. 49 (2023) 103215.
[77] M. Sobhani, H. Ajam, Experimental performance evaluation of a novel design solar desalination device equipped with air stones. Desalination 543 (2022) 116086.
[78] S. Tuly, et al., Performance investigation of active double slope solar stills incorporating internal sidewall reflector, hollow circular fins, and nanoparticle-mixed phase change material, J. Storage Mater. 55 (2022) 105660.
[79] A.K. Singh, Techno-environ-economic-energy-exergy-matrices performance analysis of evacuated annulus tube with modified parabolic concentrator assisted single slope solar desalination system. J. Clean. Prod. 332 (2022) 129996.
[80] A. Dubey, S. Kumar, A. Arora, Enviro-energy-exergo-economic analysis of ETC augmented double slope solar still with 'N' parallel tubes under forced mode: environmental and economic feasibility. J. Clean. Prod. 279 (2021) 123859.
[81] M.S. Yousef, H. Hassan, An experimental work on the performance of single slope solar still incorporated with latent heat storage system in hot climate conditions, J. Clean. Prod. 209 (2019) 1396–1410.
[82] S.W. Sharshir, et al., Factors affecting solar stills productivity and improvement techniques: a detailed review, Appl. Therm. Eng. 100 (2016) 267–284.
[83] A.J.N. Khalifa, A.M. Hamood, Effect of insulation thickness on the productivity of basin type solar stills: an experimental verification under local climate, Energ. Conver. Manage. 50 (9) (2009) 2457–2461.
[84] W. Al–Rifaie, E. Alhasat, W. Ahmed, Impact of dead seawater on the mechanical properties of ferrocement, MOJ Civil Eng 4 (5) (2018) 374–377.
[85] Laby, K. Kaye&Laby Tables of Physical & Chemical Constants. 2006-2023 [cited 2024 26 Feb 2024]; Available from: http://www.kayelaby.npl.co.uk/general_physics/2_2/2_{21.html.
[86] Madhu, B., et al., Improving performance of hemispherical solar distillation unit using paraffin wax encapsulated in waste aluminium-Cans. 2021.
[87] M. Aqib, et al., Experimental case studies of the effect of Al2O3 and MWCNTs nanoparticles on heating and cooling of PCM, Case Stud. Therm. Eng. 22 (2020) 100753.
[88] Tiwari, G.N., SOLAR ENERGY Fundamentals, Design, Modelling and Application. Revised Edition 2013 ed. 2002, 22 Delhi Medical Association Road, Daryaganj, New Delhi 110 002: N. K. Mehra for Narosa Publishing House Pvt. Ltd.

[89] M.S. Yousef, H. Hassan, H. Sekiguchi, Energy, exergy, economic and enviroeconomic (4E) analyses of solar distillation system using different absorbing materials, Appl. Therm. Eng. 150 (2019) 30–41.
[90] M.A.Z. Khan, et al., Energy, exergy, exergo-economic, enviro-economic, exergo-environmental, exergo-enviro-economic, sustainability and sensitivity (6E, 2S) analysis on single slope solar still—an experimental study, PLoS One 18 (8) (2023) e0290250.
[91] M.S. Yousef, H. Hassan, Energy payback time, exergoeconomic and enviroeconomic analyses of using thermal energy storage system with a solar desalination system: an experimental study, J. Clean. Prod. 270 (2020) 122082.
[92] S. Sharshir, et al., Thermal performance and exergy analysis of solar stills–a review, Renewable Sustainable Energy Rev. 73 (2017) 521–544.
[93] S. Shoeibi, et al., Energy matrices, exergoeconomic and enviroeconomic analysis of air-cooled and water-cooled solar still: experimental investigation and numerical simulation, Renew. Energy 171 (2021) 227–244.
[94] S.M. Parsa, et al., Energy-matrices, exergy, economic, environmental, exergoeconomic, enviroeconomic, and heat transfer (6E/HT) analysis of two passive/active solar still water desalination nearly 4000m: altitude concept, J. Clean. Prod. 261 (2020) 121243.
[95] A.E. Kabeel, A. Hamed, S. El-Agouz, Cost analysis of different solar still configurations, Energy 35 (7) (2010) 2901–2908.
[96] S.K. Nandi, H.R. Ghosh, Prospect of wind–PV-battery hybrid power system as an alternative to grid extension in Bangladesh, Energy 35 (7) (2010) 3040–3047.
[97] M.S. Yousef, H. Hassan, Assessment of different passive solar stills via exergoeconomic, exergoenvironmental, and exergoenviroeconomic approaches: a comparative study, Sol. Energy 182 (2019) 316–331.
[98] P. Pal, et al., Energy matrices, exergoeconomic and enviroeconomic analysis of modified multi–wick basin type double slope solar still, Desalination 447 (2018) 55–73.
[99] R. Hassan, H. Barua, B.K. Das, Energy, exergy, exergo-environmental, and exergetic sustainability analyses of a gas engine-based CHP system, Energy Sci. Eng. 9 (12) (2021) 2232–2251.
[100] S.W. Sharshir, et al., Energy and exergy analysis of solar stills with micro/nano particles: a comparative study, Energy Convers. Manage. 177 (2018) 363–375.
[101] S. Loem, et al., Testing of solar inverter air conditioner with PCM cool storage and sizing of photovoltaic modules, Therm. Sci. Eng. Progress 38 (2023) 101671.
[102] Holman, J.P., Experimental methods for engineers eighth edition. 2021.
[103] ISO., I. and B. OIML, Guide to the Expression of Uncertainty in Measurement. 1993: Aenor.
[104] R. Aggarwal, New correction factor for the estimation of solar radiation, J. Renewable Sustainable Energy 1 (4) (2009).
[105] Pal, P., et al., Energy matrices, exergoeconomic and enviroeconomic analysis of modified multi–wick basin type double slope solar still. 2018. **447**: p. 55-73.
[106] I. Shaheen, et al., Facile ZnO-based nanomaterial and its fabrication as a supercapacitor electrode: synthesis, characterization and electrochemical studies, RSC Adv. 11 (38) (2021) 23374–23384.
[107] Education, E. Aluminum. [cited 2023 27 September]; Available from: https://energyeducation.ca/encyclopedia/Aluminum#:~:text=The%20extraction%20of%20aluminum%20is,known%20as%20aluminum's%20embodied%20energy.
[108] K. Naveen Kishore, J. Chouhan, Embodied energy assessment and comparisons for a residential building using conventional and alternative materials in Indian context, J. Inst. Eng. Ser. A 95 (2014) 117–127.
[109] E. Ghandourah, et al., Performance enhancement and economic analysis of pyramid solar still with corrugated absorber plate and conventional solar still: a case study, Case Stud. Therm. Eng. 35 (2022) 101966.
[110] R.K. Sambare, et al., Exergy and thermo-economic analyses of various tubular solar still configurations for improved performance, Energy Sources Part A 43 (21) (2021) 2672–2691.
[111] S. Shoeibi, et al., A novel solar desalination system equipped with thermoelectric generator, reflectors and low-cost sensible energy-storage for co-production of power and drinking water, Desalination 567 (2023) 116955.
[112] R. Dhivagar, et al., Energy, exergy, economic and enviro-economic (4E) analysis of gravel coarse aggregate sensible heat storage-assisted single-slope solar still, J. Therm. Anal. Calorim. 145 (2) (2021) 475–494.
[113] D.D.W. Rufuss, et al., Effects of nanoparticle-enhanced phase change material (NPCM) on solar still productivity, J. Clean. Prod. 192 (2018) 9–29.